UNIVERSITAT POLITÈCNICA DE VALÈNCIA

School of Industrial Engineering

Development of a methodology to determine polonium-210 in different environmental matrices

Master's Thesis

Master's Degree in Chemical Engineering

AUTHOR: Belhadi , Yassine

Tutor: Carlos Alberola, Sofía

External cotutor: SAEZ MUÑOZ, MARINA

ACADEMIC YEAR: 2021/2022

CHEMICAL ENGINEERING MASTER THESIS

Development of a methodology to determine polonium-210 in different environmental matrices

AUTHOR: BELHADI YASSINE

SUPERVISOR: Carlos Alberola Sofia

Select: Sáez Muñoz Marina

Academic year: 2021-22

Acknowledgments

Abstract

This work is base on the development and validation of procedures for the determination of polonium-210 in different environmental matrices. Po-210 is an alpha-emitting isotope of the uranium-238 decay chain that occurs naturally in the environment. However, an increase in its concentration can also be present in different environmental matrices due to anthropogenic activities. Po-210 is the direct descendant of Pb-210, a beta emitter of the uranium chain used in the dating of sediments and other matrices. Therefore, the quantification of Po-210 is very useful for dating and other radioecology studies, and also for detecting possible contamination or poisoning with this radionuclide. Specifically, the work is focuse on the development of procedures for the quantification of Po-210 in aerosol filters, vegetation and soils using a sample pretreatment by microwave digestion, spontaneous deposition of polonium and measurement by alpha spectrometry. The procedures develop will be validated with reference and/or intercomparison materials available in the laboratory. For this purpose, the repeatability and accuracy of the methodology was assessed. The time needed to complete the analysis will be minimize in order to use this procedure in emergency situations.

Key Words: Polonium, environmental matrices, microwave digestion, alpha spectrometry.

Resumen

En este trabajo se plantea el desarrollo y validación de procedimientos para la determinación de polonio-210 en diferentes matrices ambientales. El Po-210 es un isótopo emisor alfa de la cadena de desintegración del uranio-238 que aparece en el medioambiente de forma natural. Sin embargo, también puede producirse un incremento de su concentración en las diferentes matrices ambientales por actividades humanas. Po-210 es el descendiente directo del Pb-210, emisor beta de la cadena del uranio que se emplea en la datación de sedimentos y otras matrices. Por tanto, la cuantificación de Po-210 es de gran utilidad para estudios de datación y otros estudios de radioecología, y también para detectar una posible contaminación o envenenamiento con este radionucleido. En concreto, el trabajo se centra en la puesta a punto de procedimientos para la cuantificación de Po-210 en filtros de aerosoles, vegetación y suelos mediante un tratamiento previo de la muestra por digestión microondas, una deposición espontánea del polonio y la medida por espectrometría alfa. Los procedimientos desarrollados se validarán con materiales de referencia y/o de intercomparación disponibles en el laboratorio. Con ello se evaluará la repetibilidad y la exactitud de la metodología. También se minimizará el tiempo necesario para completar el análisis de forma que este procedimiento pueda aplicarse en situaciones de emergencia.

Key Words: Polonio, matrices ambientales, digestión microondas, espectrometría alfa

Resum

En este treball es planteja el desenvolupament i validació de procediments per a la determinació de poloni-210 en diferents matrius ambientals. El Po-210 és un isòtop emissor alfa de la cadena de desintegració de l'urani-238 que apareix en el medioambiente de forma natural. No obstant això, també pot produir-se un increment de la seua concentració en les diferents matrius ambientals per activitats humanes. Po-210 és el descendent directe del Pb-210, emissor beta de la cadena de l'urani que s'empra en la datació de sediments i altres matrius. Per tant, la quantificació de Po-210 és de gran utilitat per a estudis de datació i altres estudis de radioecología, i també per a detectar una possible contaminació o enverinament amb este radionúclid. En concret, el treball se centra en el desenvolupament de procediments per a la quantificació de Po-210 en filtres d'aerosols, vegetació i sòls per mitjà d'un tractament previ de la mostra per digestió.

Key Words: Polonio, matrices ambientales, digestión microondas, espectrometría alfa

Contents

Chapter 4: Conclusion   69

Chapter 5: Bibliography   72

Part 2: Budget   76

Part 3: Appendix   82

List of Figures

List of Tables

Part 1: Memory

Chapter 1: Objective and Introduction

1   Objective

The objective of this work is to establish a method capable of measuring Po-210 activity in natural samples. In a first step, the work will consist in measuring the Po-210 activity in soil samples of known activity from the IAEA. This will allow to verify the functioning of the method that will be developed. In a second step, the work will consist in measuring the Po-210 activity in natural samples such as soil, aerosol, grass and tobacco samples. The objective here will be to verify whether it is possible to measure low activity using this method. The measurements obtained will be compared with other previously obtained values.

2   Introduction

The Environmental Radioactivity Laboratory (LRA[1]) is part of the Radiation Service of the Polytechnic University of Valencia and carries out different tests to measure radioactivity in different environmental matrices, in water, soil, sediments, plants, etc. In order to quantify the specific activity of a radionuclide in a non-liquid sample, it is important to put the radionuclide under study into solution. Generally, this is done using open vessel digestion methods. However, the use of these methods leads to the possibility that not all the element goes into solution. Therefore, the development of alternative processes for digesting the sample is necessary. One such alternative is the total dissolution of solid samples by microwave digestion. The application of these digestion procedures to the quantification of polonium-210 allowed the determination of the Po-210 content in the most analysed and environmentally interesting solid samples. Indeed, Po-210 is a highly radioactive, extremely volatile and toxic element. It is considered to be the most important alpha emitter in terms of internal human dose from food ingestion, which is why its analysis in environmental samples is of great importance. On the other hand, since 2007 the LRA has been accredited by the National Accreditation Body (ENAC), with the accreditation number 620/LE1050, to carry out certain tests in the field of environmental radioactivity, in accordance with the criteria established in the UNE-EN ISO/IEC 17025 standard. This accreditation confers prestige and reliability, so that by increasing the number of procedures and being accredited in them, the laboratory obtains great added value. Finally, the economic viability of this work also justifies its implementation. The laboratory already had much of the material and equipment necessary to carry out the procedure, both the microwave oven and the equipment for deposition and alpha spectrometry. Only the cost of the reagents and some of the additional materials used and the wear and tear on the equipment are charged to the laboratory, allowing the research project to be carried out successfully. [1]

3   Motivation

The motivation for this work comes from the UN Member States' Sustainable Development Programme. It is a project for peace and prosperity for humanity and the planet for today and tomorrow. The programme is structured around 17 sustainable development goals established by UN member states. These goals emphasise that eradicating poverty and other deprivations must go hand in hand with strategies to improve health and education, reduce inequality and

---

[1]LRA means in Spanish, Laboratorio de Radioactividad Ambiental

stimulate economic growth, while tackling climate change and working to preserve our oceans and forests [2]. All of these goals are shown in Figure 1.

Figure 1: Sustainable Development Goals [2]

This work attempts to implement objectives 3 and 15. Goal 3 is good health and well-being for all. Po-210 is highly radiotoxic to the human body. It is therefore very important to measure it and to follow a set of guidelines in order to avoid contamination of the public or workers who come into contact with this radioactive element. Objective 15 is to preserve terrestrial life and ecosystems. Indeed, Po-210 can be found in nature due to human activity. Po-210 is therefore found in nature and can potentially contaminate certain plants and animals. As for humans, Po-210 is very toxic for animals. To avoid this problem, a set of guidelines has also been put in place. Measuring Po-210 in natural samples makes it possible to see whether these guidelines (exemption limits) are respected. These measurements can also be used to check whether some of the samples are contaminated or not [2].

4 Radioactivity

Any unstable nuclide aims to become stable. Therefore, an unstable nuclide will undergo a spontaneous nuclear decay reaction in order to transform itself into a stable element [3]. This is radioactivity. During decay, the unstable nuclide emits radiation, the nature of which depends on the type of decay. It is also possible that the nuclide resulting from the decay may be unstable, leading to a further decay and so on until a stable nuclide is obtained. The term decay chain is used for such a phenomenon. In nature, there are mainly four types of decay classified according to the type of particle emitted:

- Alpha decay

- Beta decay itself is divided into three sub-categories

- Gamma decay

- Fission

The stability of a nuclide depends on the nuclear binding energy. The higher the nuclear binding energy, the more stable the nuclide. The Segre diagram in the Figure 2 shows that the ratio between the number of neutrons (N = A-Z) and the number of protons (Z) is close to 1 for light nuclei such as oxygen. On the other hand, the heavier a nucleus is, the higher the number of N is than the number of Z. This means that stability for heavy nuclei is achieved for higher N numbers, as is the case for bismuth. The Segre diagram shows that the stability zone moves away from the straight line of ratio 1 between N and Z. This excess of neutrons in heavy nuclei compensates for the strong repulsion between protons. However, after a certain threshold, the additional neutrons are no longer able to stabilise the nucleus. In fact, all isotopes of elements with an atomic number of 84 or more can be considered radioactive, as is the case with polonium. These very heavy nuclei disintegrate spontaneously [3].
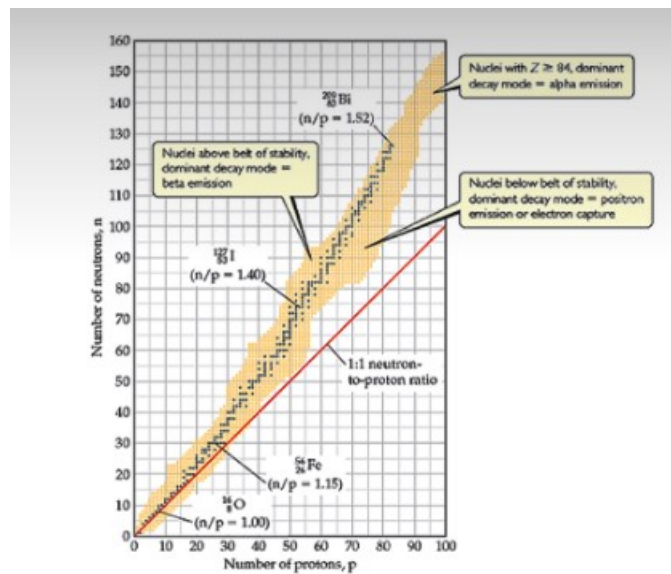
Figure 2: Segre diagram [4]

4.1 Type of decay

As mentioned above, the type of decay depends on the type of particle emitted during the decay. From the diagram in the Figure 3 it can be seen that the type of decay also depends on the type of nucleus [3]. Indeed, alpha decays and fission occur for very heavy nuclei as shown in the diagram. Beta decays occur for lighter nuclei even if some heavy nucleus also follows this type of decay. The diagram shows that β^- decay occurs for nuclei above the stability zone while β^+ decays occur for nuclei below the stability zone.
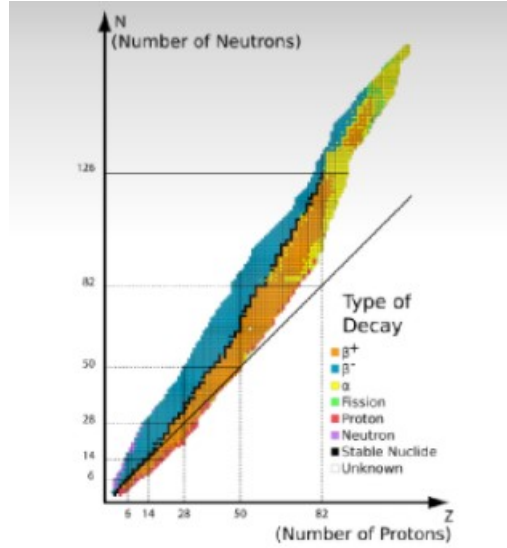
Figure 3: Segre diagram 2 [4]

4.1.1 Alpha decay

As mentioned above, alpha decay generally occurs for unstable heavy nuclei (A>140) such as Po-210. Alpha decay is a spontaneous separation from the rest of the nucleus of two protons and two neutrons bound in the form of a He nucleus as shown in the equation 1. These nuclei decay into lighter nuclei.

$$
{}_{Z}^{A}X_{N} \longrightarrow {}_{Z-2}^{A-4}Y_{N-2} + \alpha({}_{2}^{4}He^{2+}) \tag{1}
$$
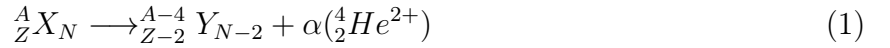
4.1.2 Beta decay

Decay is the most common type of decay encountered as shown in the diagram in Figure 3. Beta decay is a process due to the weak interaction in which a proton is converted to a neutron or a neutron to a proton in order to reach a stable state. During decay, the unstable nucleus emits either an electron (e^-) or a positron (e^+). The aim of this decay is to optimise the neutron-proton ratio in order to reach the stable state. Depending on the charge emitted, the decay is classified as either β^+ when an e^+ is emitted or β^- when an e^- is emitted. It is also possible to have an electron capture when a proton recombines with an electron to form a neutron. The electrons and or positrons emitted during β radioactivity do not pre-exist in the nucleus but are created from energy during decay. [3] [2]

The β^- decay occurs when there is an excess of neutrons in the unstable nucleus (position above the stability zone in Figure 2). In order to compensate for this excess of neutrons, a neutron (n) in the unstable nucleus decays to give rise to a proton (p+) and an electron (e^-) as shown in the equation 2. This decay will also give rise to an electron antineutrino ($\widetilde{\nu}$) in order

---

[2]Positronic capture is also possible when a neutron and a positron combine. However, positron capture is not observed experimentally due to the absence of free positrons in stable matter and the low probability of weak processes.

to respect the conservation laws [3].

$$n \longrightarrow p^+ + e^- + \widetilde{\nu}$$
$$_Z^A X \longrightarrow_{Z+1}^A Y + \beta^- + \widetilde{\nu} \tag{2}$$

The β^+ decay occurs when there is an excess of protons in the unstable nucleus (position below the stability zone in Figure 2). In order to compensate for this excess of proton, a proton (p^+) in the unstable nucleus decays to give rise to a neutron (n) and a positron (e^+) as shown in the equation 3. This decay will also give rise to an electron neutrino (ν) in order to respect the conservation laws [3].

$$p^+ \longrightarrow n + e^+ + \nu$$
$$_Z^A X \longrightarrow_{Z-1}^A Y + \beta^+ + \nu \tag{3}$$

Electron capture competes with β^+ decay. It also occurs when there is an excess of protons in the unstable nucleus. During electron capture, a proton (p^+) will combine with an electron (e^-) to give rise to a neutron (n) followed by a neutrino as shown in equation 4. This process is not considered a radioactive transition despite its slight resemblance to β^+ decay [3].

$$p^+ + e^- \longrightarrow n + \nu$$
$$_Z^A X + e^- \longrightarrow_{Z-1}^A Y + \nu \tag{4}$$

4.1.3 Gamma decay

Gamma decay is a process of radioactive decay of an excited element with the emission of a high-energy photon, also called gamma radiation. Gamma emissions are electromagnetic waves with high penetrating power. The equation 5 shows the gamma decay of an excited element (X^*). This element will de-excite (X) by emitting gamma radiation (or photon). Gamma emission is considered the most dangerous of the different types of radioactive decay from the point of view of external radiation because of its long path through matter [3].

$$_Z^A X^* \longrightarrow_Z^A X + \gamma \tag{5}$$

4.1.4 Fission

Fission is a decay process consisting of the division of a heavy nucleus into two or more equally heavy fragments (less heavy than the nucleus undergoing fission) accompanied by the emission of one or more neutrons as shown in Figure4 . Fission is a phenomenon similar to alpha decay but more complex and rare. This decay process is used in nuclear reactors [3].
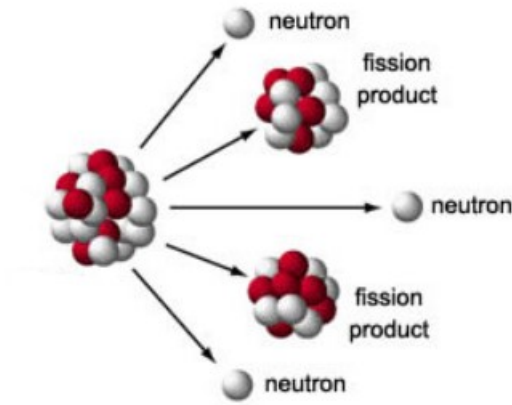
Figure 4: Fission scheme [4]

4.2 Law of decay

The activity of a radioactive isotope is defined as its number of decays per second and is given by the fundamental law of radioactive decay represented by the equation 6 [3] :

$$A = \frac{dN}{dt} = -\lambda N \tag{6}$$

Where:

- A = activity [Bq]

- N = the number of radioactive nuclei

- λ = the decay constant [s^{-1}]

- t = the time [s]

By integrating the equation 6 for a time t = 0 and N = N_0 where N_0 is the number of initial nuclei of a given radioactive substance, the exponential decay equation is obtained.

$$
\begin{aligned}
dN &= \int_0^t -\lambda N dt \\
N &= N_0 e^{-\lambda t} \\
A &= A_0 e^{-\lambda t}
\end{aligned}
\tag{7}
$$

The unit of activity is usually expressed in Becquerel (Bq) but can also be given in Curie (Ci) which is the historical unit. The unit of Curie is by definition the best available estimate of the activity of a gram of pure Ra-226. The equation 8 gives the conversion between Bq and Ci. At its 1975 meeting, the General Conference on Weights and Measures (CGPM) adopted a resolution declaring that the becquerel, defined as one disintegration per second, has become the standard unit of activity [3].

$$1 Bq = 2.703 * 10^{-11} Ci \tag{8}$$

The decay constant (λ [s^{-1}]) is also an important parameter of the radio activity of a radio isotope. This constant indicates the decay probability of a radio isotope per unit time. This constant is a characteristic of each radioisotope. Another constant often used and related to λ is the half-life time,($T_{1/2}$ [s]) of a radioisotope. This is the time required for the initial activity of a radioisotope to be halved. The equation 9 shows the link between the decay constant and the half-life of a radioisotope [3].

$$T1/2 = \frac{ln2}{\lambda} \tag{9}$$

The graph in the Figure 5 shows the evolution of the number of radioactive nuclei as a function of time at given half-lives. As the equation 7 indicates, the graph has the shape of a decreasing exponential, showing that after a period T (which represents a half-life) half of the radioactive nuclei have disappeared.
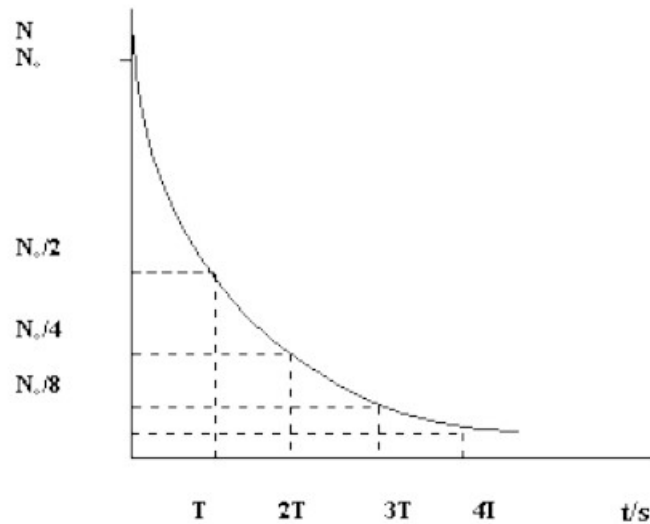
Figure 5: Evolution of the number of radioactive nuclei as a function of time at given half-lives

4.3 Secular equilibrium

By definition, a radioactive isotope is in secular equilibrium if its quantity is constant over time. This will be the case if the rate of creation of this radioisotope (daughter), by the decay of its father, is equal to the rate of its own decay [5].

The rate of decay per unit time (activity) of an isotope is directly proportional to its quantity N as shown by the equation 10.

$$\frac{dN}{dt} = -\lambda N = A(t) \tag{10}$$

With λ is the decay constant of the isotope [s^{-1}].

Considering N_1 the number of father atoms and N_2 the number of daughter atoms, the activity of the father is given by $\lambda_1 N_1$ and the activity of the daughter by $\lambda_2 N_2$. Since the daughter atoms come from the decay of the father atoms and can also decay (if the daughter atoms are also radioisotopes), the quantity of daughter atom N_2 will be equal to the difference

between the rate of creation by the father and the rate of decay of the daughter. By noting $\frac{dN_2}{dt}$ the variation of the number of atoms N_2 with time, the equation 11 is obtained:

$$\frac{dN_2}{dt} = \lambda_1 N_1 - \lambda_2 N_2 \tag{11}$$

This equation means that if N_2 is produced faster than it decays, the quantity N_2 will increase. On the other hand, if N_2 decays faster than it is produced, the system will tend towards an equilibrium since, in order for N_2 radioisotopes to decay, they must first be produced by the decay of the parent. To reach this equilibrium, it is necessary that $\lambda_2 >> \lambda_1$. Generally it is considered that equilibrium is reached in the case where $\lambda_2 \geq 10\lambda_1$. When secular equilibrium is reached, the quantity of N_2 with respect to time is constant. The equation 11 thus becomes:

$$\frac{dN_2}{dt} = 0 = \lambda_1 N_1 - \lambda_2 N_2 \tag{12}$$

$$\lambda_1 N_1 = \lambda_2 N_2 \tag{13}$$

$$A_2 = A_1 \tag{14}$$

It is therefore possible to calculate the daughter's activity from the father's activity if the secular equilibrium is reached [5].

5   Polonium

In 1898, Pierre and Marie Curie discovered polonium during their studies of radioactive elements in minerals. Their study involved the analysis of a uranium-rich ore called pitchblende. They noticed that pitchblende was four times more active than metallic uranium and therefore concluded that another, much more active element other than uranium, was present in the ore [6]. In order to isolate this unknown element, a rather complex set of steps for chemical separation had to be developed. This previously unreported metal was named polonium like the Curie s' home country. Thanks to this discovery, Marie Curie was awarded the Nobel Prize in Chemistry in 1911 [7].

The atomic number of polonium is 84 and it belongs to group 16 of the periodic table of elements (chalcogen) as do oxygen, sulphur, selenium and tellurium. This element has physico-chemical properties intermediate between metals and non-metals. It is therefore considered a metalloid. Its stable oxidation states are as follows: $-II$, $+II$, $+IV$, and $+VI$. In aqueous solution, the $+IV$ oxidation state is the most stable in the form of polonate ions PoO_3^{2-}.

It has 33 known isotopes with the particularity that all of these are radioactive. There are 7 naturally occurring radioactive isotopes of polonium while the other isotopes are all derived from the decay chain of natural long-lived radionuclides such as uranium-238, uranium-235 and thorium-232 shown in Figure 6 :
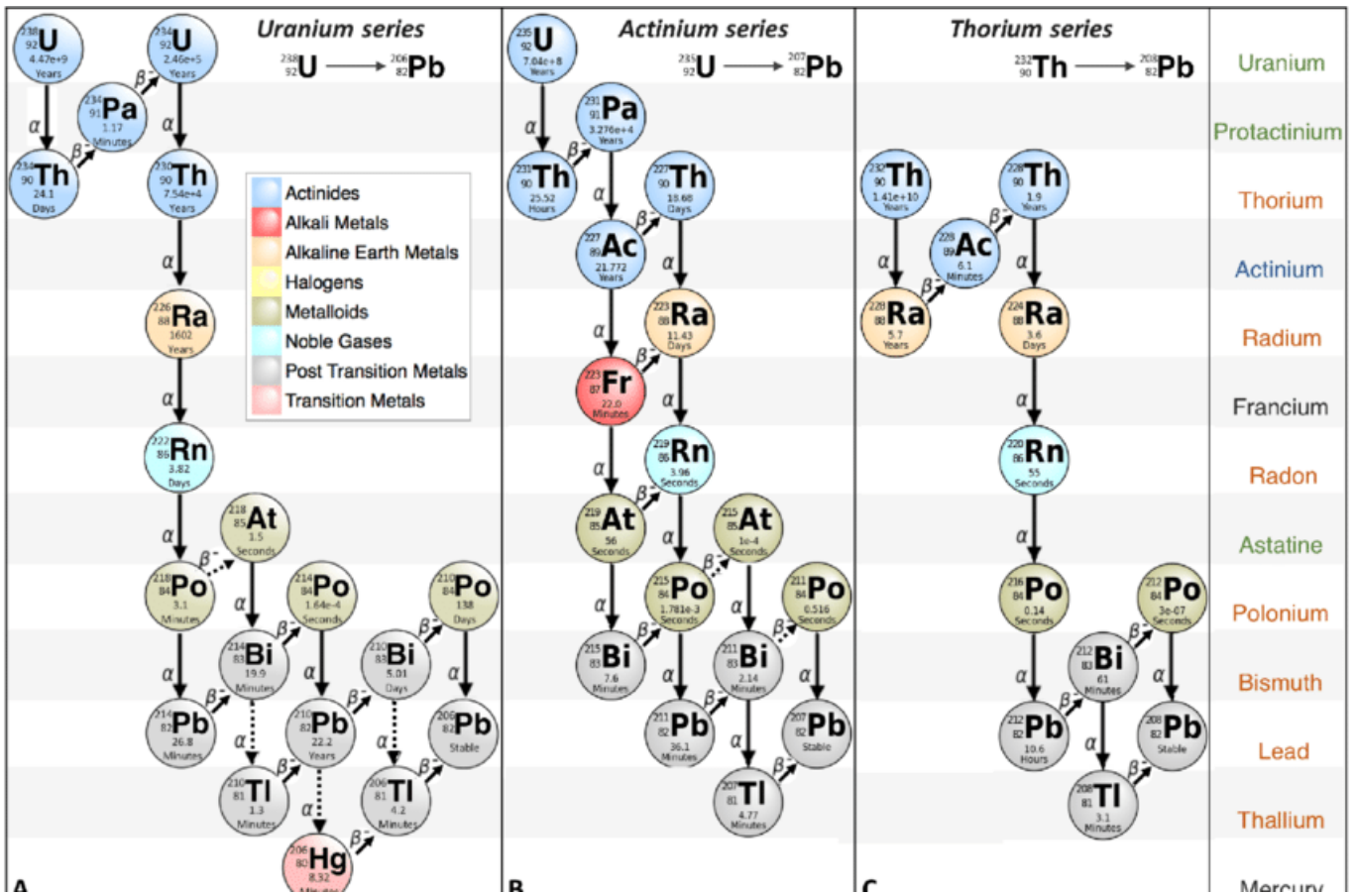
Figure 6: Radioactive decay chain series of U-238, U-235 and Th-232 [8]

Looking at the decay chain of these three elements, it is remarkable that :

- Po-210, Po-214 and Po-218 are part of the uranium-238 decay chain

- Po-211 and Po-215 are part of the uranium-235 decay chain

- Po-212 and Po-216 are part of the thorium-232 decay chain

Of all these elements, Po-210 is the most naturally abundant. It is an alpha emitter with a half-life of 138.4 days. In the same decay chain, Po-214 and Po-218 are also alpha emitters but their respective half-lives are much shorter. Among the artificial isotopes, only two are of interest. These are Po-208 and Po-209, whose half-life is greater than one day. These two elements are often used as tracers in radiochemical analysis, as will be the case in this work. Generally, the use of Po-209 is preferred to that of Po-208 because Po-209 has a very distinct alpha emission line compared to Po-210 and has longer half-life. Table 1 shows the different characteristics of Po-208, Po-209 and Po-210.

Table 1: Relevant decay data for ^{208}Po, ^{209}Po, ^{210}Po [9]

Radionuclide	Half-life ($T_{1/2}$)	Disintegration modes	E_α (MeV)	Intensity (%)
^{208}Po	2,898 y	α 99,99777%	5,115	99,9956
			4,220	2,4*10^{-4}
		ϵ 0,00223%		
^{209}Po	102 y	α 99,52%	4,885	20
			4,883	80
			4,622	0,551
			4,310	1,5*10^{-4}
			4,110	5,6*10^{-4}
		ϵ 0,48%		
^{210}Po	138,376 d	α 100%	5,304	100
			4,517	1,22*10^{-3}

5.1 Origin of polonium-210

Polonium-210 can occur either naturally in the environment as a result of the decay of natural uranium or artificially in a nuclear reactor or cyclotron. Polonium-210 can be produced via a nuclear reactor by neutron bombardment of Bi-209, generating Bi-210, which has a half-life of five days and which transforms, by β^- emission into Po-210 as shown in Equation 15 [10].

$$^{209}_{83}\text{Bi} \xrightarrow{\text{n},\gamma} {}^{210}_{83}\text{Bi} \xrightarrow{\beta^-} {}^{210}_{84}\text{Po} \tag{15}$$
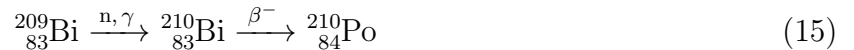
Polonium-210 can also be produced in cyclotrons via the direct ^{209}Bi (α, t) ^{210}Po and ^{209}Bi (α, p2n) ^{210}Po reactions [11].

Naturally occurring polonium will be further detailed in the following sub-section as almost all samples analysed in this work are of natural origin and are probably contaminated with naturally occurring Po-210.

5.1.1 Naturally occurring polonium :

As mentioned above, naturally occurring polonium-210 comes exclusively from the decay of uranium-238, which makes natural Po-210 a naturally radioactive element. Po-210 can be found in the atmosphere, oceans, soil, rocks and other natural elements.

5.1.1.1 Polonium in the atmosphere

The main sources of polonium-210 in the atmosphere are [12] :

- The exhalation of radon-222, also from the decay of uranium-238, from the surface layers of the earth's crust is the main source of atmospheric Po-210. The radon-222 in the air will then decay to Pb-210 which will decay to Bi-210 which will give rise to Po-210.

- The contribution of stratospheric aerosols containing Po-210 contaminating the lower atmospheric layers (1 to 5%).

- Volcanic emissions, which are believed to be the source of about 50% of the Po-210 present in the lower layers of the atmosphere.

- Anthropogenic activities, which will be described later.

Po-210 is often found attached to aerosols in the atmosphere because lead and bismuth are likely to attach rapidly to them. The atmospheric residence time of Po-210 varies between 15 and 75 days with an average value of around 26 days [13]. Depending on the climatic and geographical situation, these contaminated aerosols fall back to the surface of the land and oceans as dry or wet deposition. Wet deposition is the removal of atmospheric constituents to the ground surface by precipitation such as rain, snow and hail. Indeed, during atmospheric precipitation, the different elements such as Pb-210, Bi-210 and Po-210 present on the aerosols will either be captured by the raindrops during their fall (wash out) or will be found in a supersaturated air mass serving as condensation nuclei and will thus be directly incorporated in the raindrops (rain out). Wet deposition is the main deposition process of atmospheric Po-210. Dry deposition consists of resuspended dust deposits and fine particles falling down due to the gravity [14].

5.1.1.2 Polonium in soils

Soils represent the interface between the atmosphere, the parent rocks and the underground hydrological system. Soils are not homogeneous environments. They are differentiated into several horizons with their own physical, chemical and biological characteristics. These characteristics have consequences on the retention of metals in the soil horizons, their mobility and bioavailability [15]. For soils, the presence of Po-210 is mainly due to the presence of uranium-238 in the soil and atmospheric fallout. The latter will be found either in the crystalline matrix present in the soil or at the surface of the earth due to the exhalation of radon by diffusion. Compared to uranium-238, polonium-210 is present in extremely small quantities due to its short half-life (compared to uranium-238). As an example, the average concentration of uranium-238 in soil is 2,7 ppm and 0,20 ng for Po-210 per tonne of soil [14]. The sources of Po-210 activity can be separated into two parts, supported Po-210 and unsupported Po-210.

Supported Po-210 results from uranium-238 present in soils and sediments. Theoretically, Po-210 and Pb-210 should be in secular equilibrium with U-238 in unweathered rocks. However, this equilibrium between radionuclides can be disturbed by geomorphological and geochemical phenomena that will modify the uranium concentration. Moreover, the particular physical state of radon-222 (radioactive gas) also leads to a disruption of the secular equilibrium between the radionuclides of the uranium-238 family, including polonium-210. Unsupported Po-210 comes from atmospheric fallout. Po-210 is deposited and accumulates on the surface of the earth and plants. Due to atmospheric deposition, the activity of Po-210 in surface soils is systematically higher than in deeper layers. The equilibrium between radionuclides in the uranium-238 family could not be maintained due to preferential leaching of radionuclides and the release of radon from the upper soil layers into the atmosphere [16]. The diagram in Figure 7 helps to visualise the two types of sources of Po-210 activity in soils.
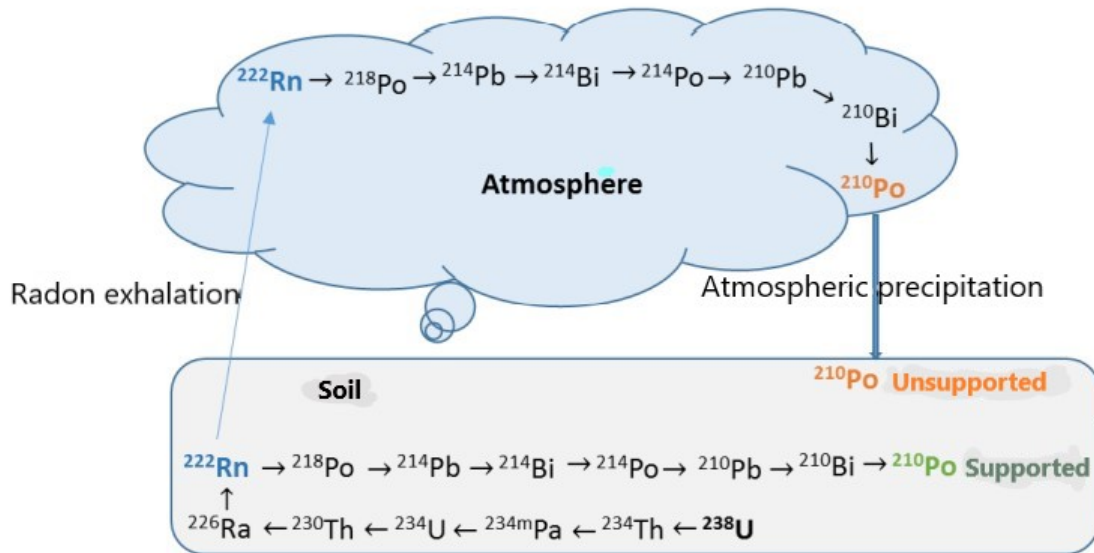
Figure 7: Schematic representation of the dual origin of Po-210 in the soil.[17]

5.1.1.3 Polonium in the marine environment

In the marine environment, Po-210 is produced by the decay of Pb-210, which is itself the offspring of Ra-226 dissolved in seawater. It also comes from atmospheric fallout as mentioned above. In addition, the release of phosphogypsum waste from phosphate fertiliser factories leads to increased concentrations of polonium-210 in the sea.

5.1.1.4 Polonium in vegetation

In areas far from any anthropogenic activity, the mass activity of Po-210 in plants varies between 0.1 and 160 Bq/kg. The Po-210 present comes mainly from atmospheric fallout (dry or wet) and from the resuspension of particles present on the soil. Foliar transfer is therefore the main route of contamination of plants. Root transfer is also possible but is much weaker compared to foliar transfer[18]. A study shows that the mass activity is higher by a factor of 5 in the foliage of the plants analyzed than in their roots [18]. They also showed that polonium is more concentrated in tobacco leaves.

The transfer of polonium to animals is also possible. Indeed, if a herbivore feeds on grass containing a certain activity in Po-210, it is possible to have a transfer. In mammals, the mass activity of Po-210 is generally higher in the viscera and bones than in the muscles, while in poultry, the liver and gizzard concentrate the polonium [18]. The Figure 8 summarizes the entire natural pathway of Po-210 in the environment.
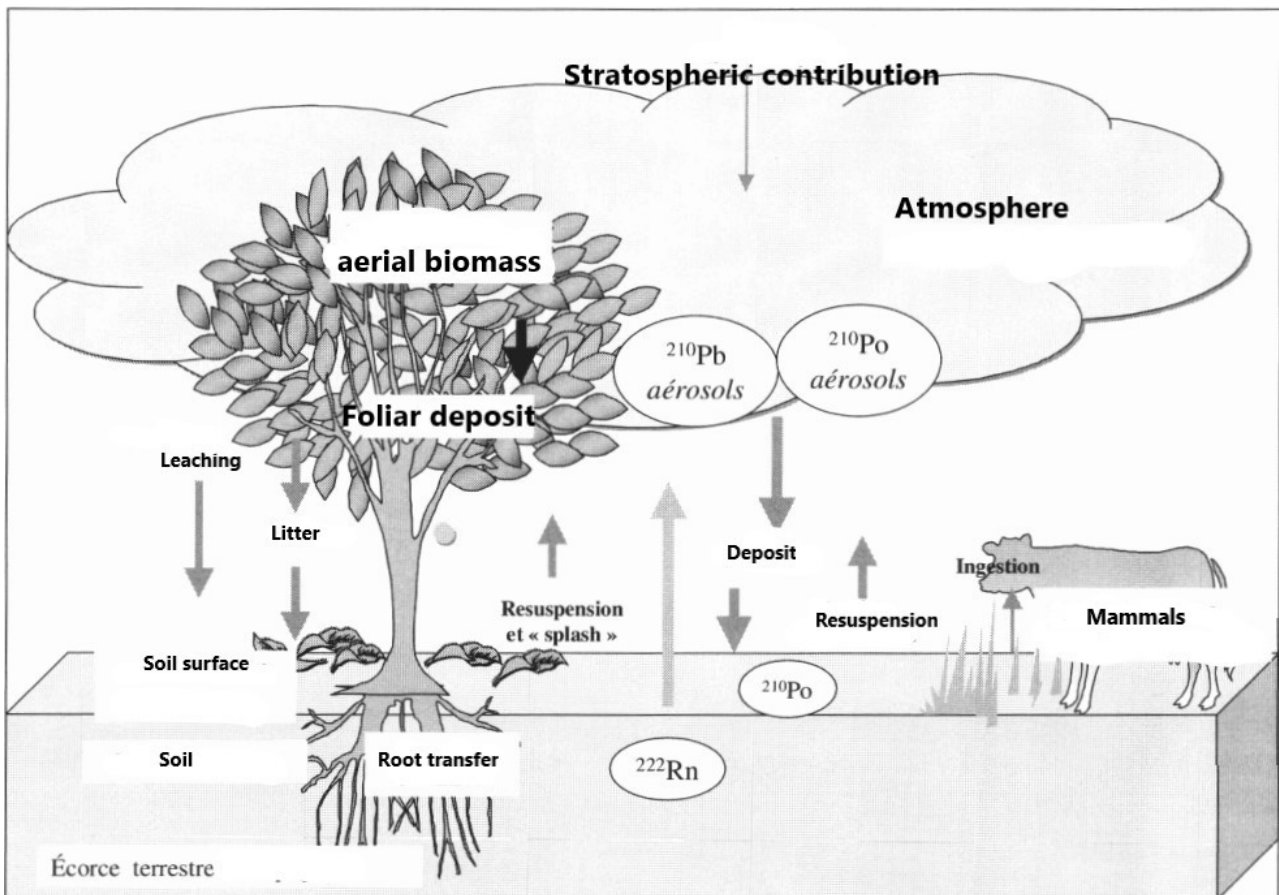
Figure 8: Main transfer pathways of Po-210 in terrestrial environment [18]

5.1.2 Po-210 from anthropogenic activities

Another element to be taken into account when analysing the presence of Po-210 in nature is anthropogenic activity, which can indirectly increase local concentrations of Po-210 in the air very strongly. One of the findings that has been made previously is that anthropogenic activity is one of the main causes of the increase of polonium concentration in nature. It is therefore interesting to understand how these activities contribute to this. The two main anthropogenic activities causing the increase of Po-210 in nature are the phosphate fertiliser and phosphoric acid industries and uranium ore mining. Mining and drilling activities significantly increase the concentration of Po-210 in the air. According to UNSCEAR, annual global atmospheric releases of Po-210 linked to human activities are of the order of 660 GBq per year , including 490 GBq per year from the phosphate industry, which accounts for a large proportion of Po-210 emissions into the air [19]. It is also necessary to take into account the uranium mines, which are the source of overconcentrations of polonium in their vicinity.

5.1.2.1 Po-210 from the phosphate fertiliser industry

In order to manufacture phosphoric acid and chemical fertilisers, industries have started using phosphate rock. These phosphate rocks contain many heavy metals such as Hg, Cd, As, Pb, Cu, Ni and Cu as well as natural radionuclides such as U-238, Th-232 and Po-210 [20]. Therefore, the extraction and processing of these rocks releases radionuclides into nature through end products such as phosphate fertilizers and phosphoric acid. They are therefore considered a potential source of contamination by natural radionuclides and heavy metals [17]. During their

15

production, radionuclides migrate according to their solubility, e.g. uranium isotopes form highly soluble compounds with phosphate ions, while radium, lead and polonium isotopes are concentrated in the by-product phosphogypsum ($CaSO_4.2H_2O$) [17]. It have be shown that Po-210 activity in phosphogypsum samples from the four main phosphoric acid producers in Brazil varies from 53 to 667 Bq/kg [17]. Therefore, the relatively high use of phosphate fertilizers in agricultural crops may increase the level of Po-210 not only in soils, but also in plants.

In the south of Spain (Andalucia), the region of Huelva had a phosphate fertilizer industry. Despite the closure of the plant, a huge amount of radioactive elements such as Po-210 were released. This has resulted in an increase in the average Po-210 activity in the area.

5.1.2.2 Po-210 from uranium ore mining.

Since Po-210 is present in the decay chain of uranium-238, it is quite normal that Po-210 is released into nature during uranium mining. The operation of these mines is therefore a major source of environmental contamination. In the vicinity of former uranium mining sites, natural systems such as soils, sediments and especially wetlands trap significant amounts of uranium [17]. In the United States, measurements in soil and vegetation near a uranium mine showed that average Po-210 concentrations were 30 kBq/kg and were generally higher than the natural geological background concentration (0,8 kBq/kg) [17]. In Spain, some areas have uranium-rich soils as shown in Figure 9 [21]. The map in the Figure 9 shows that the Central Iberian area and the Galicia area have a high concentration of uranium in soil and sediments compared to other areas of Spain [22].
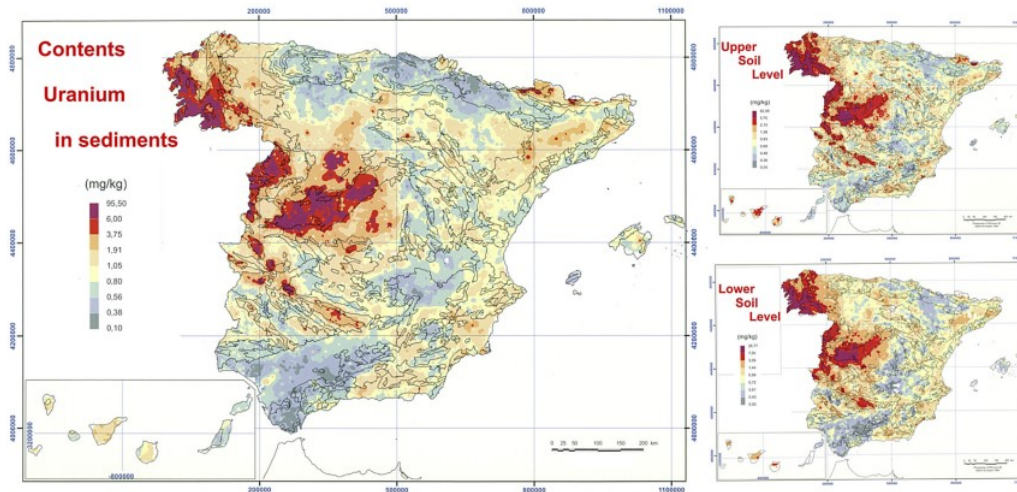
Figure 9: Distribution of uranium in sediments (left) and soils of the Spain (right) [22]

This high concentration is explained by the geological nature of the soil as shown on the geological map of Spain in Figure 10. This map shows that the soil in these areas of high uranium concentration is granitic [23]. Granitic soils are known to be rich in pitchblende, which is rich in uranium. Therefore, the probability of having Po-210 released into the environment in these areas is much higher than in other areas of Spain [21].
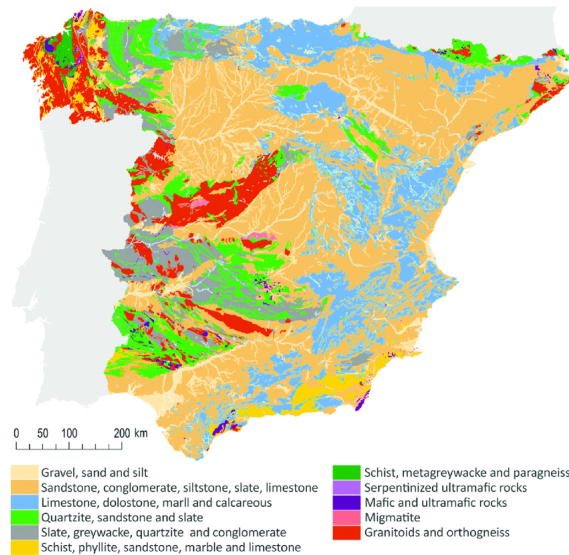
Figure 10: Influence of environmental factors and spatial distribution. [23]

5.2 Radiotoxicity of Po-210

The study of Po-210 in nature is very important because Po-210 is extremely toxic to humans. A few micrograms are sufficient to cause death [17]. Po-210 is about one million times more toxic than cyanide [17]. Po-210 is an alpha emitter with an energy of approximately 5,304 MeV. Alpha emitters have a very short average path through the air and are stopped by a single sheet of paper. The risk of external contamination is therefore very low. However, in the case of internal contamination, Po-210 does enormous damage to the human body. Internal contamination can be caused by ingestion, inhalation, injection or direct skin contact with Po-210. Once present in the body, alpha particles do 20 times more damage than X-rays or gamma radiation. In water, the linear energy transfer (LET) of Po-210 is about 100 keV/m and its average distance is 50 µm. The human body is 70% water, so the TEL of Po-210 in biological media is close to that of water, allowing alpha radiation in the body to penetrate human cells of about 10 and 30 µm in diameter [17]. These alpha particles will cause DNA breaks resulting in cellular damage which in turn causes both mutagenic and cytotoxic effects. In addition, some experience suggests that the bystander effect, caused by contaminated cells, also affects neighbouring non-irradiated cells [17]. Furthermore, ingested polonium is more easily absorbed into the bloodstream than some other α-emitting radionuclides, such as plutonium-239. Polonium-210 that enters the bloodstream is deposited mainly in soft tissues, with the highest concentrations in the reticuloendothelial system, mainly the liver, spleen and bone marrow, as well as in the kidneys and skin, particularly the hair follicles [17].

Radiation at sufficiently high doses is lethal within days or weeks, due to the massive destruction of cells in the organs and tissues of the body. Bone marrow tissue is particularly sensitive, followed by the epithelial lining of the digestive tract [17]. The median lethal dose (LD50), which is the mass of substance that must be ingested to have a 50% death rate in the study population, for an acute radiation exposure is approximately 4 Sv, which is roughly equivalent to ingesting 50 ng or inhaling 10 ng of polonium-210 [17]. This is a method to measure the short-term toxic potential of a substance. Another interesting value is that the measured concentration of Po-210 in the lung parenchyma of smokers is about three times higher than that of non-smokers [17], which makes the analysis of tobacco samples very interesting.

Detection of Po-210 in the human body is not easily achieved by standard techniques because alpha particles in the body cannot pass through the skin from inside to outside. Specific detection of α-particles in a patient's urine or stool is necessary [17].

5.3 Regulation of Po-210

As polonium is dangerous to humans, a European directive was issued on 5 December 2013. This is the COUNCIL DIRECTIVE 2013/59/EURATOM laying down basic safety standards for health protection against the dangers arising from exposure to ionising radiation and repealing Directives 89/618/Euratom, 90/641/Euratom, 96/29/Euratom, 97/43/Euratom and 2003/122/Euratom [24]. This directive includes a set of decisions in the management of radionuclides of natural origin. It imposes a set of rules on industrial sectors that use natural radioactive materials, such as the production of phosphate fertilisers. In particular, these industries must comply with a set of guidelines involving radiation protection, personnel dose and exemption limits. Listing all of these guidelines would be very time consuming and beyond the scope of this work. All the directives can be found in the Directive 2013/59/EURATOM. Only the exemption value is of interest in this case. Indeed, this exemption value will influence the measurements made on natural samples. The exemption value of Po-210 depends on whether it is in secular equilibrium with U-238 or not. If Po-210 is in equilibrium, the exemption value is 1 kBq/kg. If it is not, the exemption value is 10 kBq/kg [24].

6 Treatment of the samples

The samples studied in this work were taken from the environment, such as soil, plant, tobacco, aerosol, etc. The amount of polonium-210 in these elements is small. Furthermore, alpha radiation has a very short average path through the material and can be easily stopped with a sheet of paper. This means that the sample matrix must be removed first. It is also possible that other alpha emitter elements are present in the samples. Therefore it is also important to find a method to isolate the polonium present in the sample after destruction of the matrix.

This section will be separated in two part. The first part will describe in a theoretical way the different possibilities of digestion methods that are usually used to remove the matrix from the natural sample and to put the desired analytes into solution. The second part will consist of a theoretical description of the main separation methods commonly used in the scientific field.

6.1 Digestion

The main purpose of digestion is to allow the dissolution of natural samples while keeping the elements of interest. The dissolution of samples was already used in Ancient Greece and Egypt to control the purity of gold and silver. In the 14th century, the discovery of mineral acids provided the basis for the industrial method of separating gold and silver, as the accuracy and speed of these preparations improved [25]. It should be noted that the sample digestion step is quite complex and is one of the biggest challenges in the process of measuring Po-210 in natural samples. Indeed, these samples are composed of unknown elements such as organic constituents. The aim of digestion is to bring the element of interest, in this case Po-210,

into solution in a solid or non-aqueous sample. A good digestion makes the separation and analysis as optimal as possible. Since very few natural or organic materials are water soluble, these materials commonly require the use of acids or molten salts to bring them into solution. These reagents normally reach the solution by an oxidation-reduction process that leaves the constituents in a more soluble form. In wet processes, there are three methods commonly used for the decomposition of natural samples. These methods produce an aqueous solution containing the analyte to be analysed and are listed here:

- Open vessel acid digestion.

- Fusion in a molten salt medium.

- Acid digestion in a closed vessel using a microwave oven.

These methods differ in the use of reagents and the temperature at which the decomposition is carried out. However, whichever method is used, it must always be carried out avoiding any type of contamination and retaining the analytes in the inorganic residue [26]. A key factor in the preparation and analysis of natural samples is the care needed to avoid losses of polonium due to its volatilisation. The amount lost can vary depending on the chemical form of the polonium: organic complexes and halides are known to be particularly volatile [27].

6.1.1 Open vessel acid digestion

Open vessel acid digestion involves placing the sample in an acid mixture and heating it using a hot plate, oven, Bunsen burner or muffle. For environmental analysis, the use of an acid mixture that may contain nitric acid, hydrochloric acid, hydrofluoric acid and perchloric acid is most commonly used. Each of these acids has a defined role in dissolving the sample. Nitric acid acts as an oxidising agent while hydrochloric acid provides complexing properties [28]. Hydrofluoric acid is generally used to break down silicate-rich soil samples. Perchloric acid has a similar role to nitric acid but is more expensive and can be dangerous if the sample is rich in organic matter (risk of explosion). It is also possible to replace nitric acid with sulphuric acid for organic samples as nitric acid sometimes does not reach a sufficient temperature to destroy the last traces of organic matter in the sample although it is able to decompose most of the sample. In order to increase the solubilisation capacity of the acids used, bromine or hydrogen peroxide is sometimes used.

Digestion is usually carried out in an open heated vessel under a fume hood to avoid inhalation of acid vapour. Convection is used to transfer heat to the solution directly in contact with the heat source. An important parameter to consider is the boiling point of the different acids used. This is the parameter taken as a reference during open digestion as it allows the maximum temperature to be reached before volatile losses of acids, thus allowing the quantity of acid to be used in the mixture to be optimised. This method has many shortcomings, especially when determining Po-210 in natural samples. Indeed, to avoid loss of Po-210 it is very important to stay below 150°C [9]. The risk of losing Polonium during open digestion is high and the boiling point of the solution becomes a limiting factor for the maximum temperature that can be reached. In addition, the decomposition of the sample by this method requires a very long time (from a few hours to a few days). This method also requires a large amount of reagent. All these defects make the closed digestion process with the use of a microwave preferred because this method allows to erase these defects.

6.1.2 Fusion digestion

Fusion digestion is used when samples are much more difficult to dissolve with acids, such as in the case of sludge, soil and rock samples. The principle of this method is to mix an aliquot of the sample with a salt and heat the mixture to temperatures above the melting temperature of the salt. Once the mixture has melted, it is cooled to room temperature. This process can be repeated several times if the sample is not completely dissolved. In the case of the determination of Po-210 in natural samples, the salt most often used is Na_2CO_3 because it is able to transform oxides into soluble sodium salts [29]. Sometimes a sodium oxide is added in addition to the salt to allow optimal decomposition of oxide-poor samples. Indeed, it is important that the samples contain chemically bound oxygen, which is not always the case. Therefore, the addition of sodium oxide before melting becomes relevant and helps the digestion process of low-oxide samples. During melting, the temperature to be reached is 600°C [29]. This is problematic due to the volatile nature of Polonium. This method is therefore generally used when the samples are extremely difficult to dissolve.

6.1.3 Closed vessel microwave digestion

Since the beginning of the 19th century, many methods of sample preparation have been developed. Nowadays, technologies have evolved to the point where detection limits in the ppb range can be achieved. However, the development of these processing techniques has not been as rapid. In order to convert solid samples into homogeneous solutions, chemists have resorted to time-consuming extraction methods that require continuous control by the analyst and carry the risk of possible contamination of the sample. The use of microwave ovens in the digestion of samples led to a great improvement in the field of radiochemistry in the 1975s. It is a method of processing samples quickly and efficiently. Heating in a microwave oven allows for better control of the process. The first biological sample to be processed by this method was made in 1975 using a domestic microwave oven. This oven was used to heat a mixture of acids placed in an Erlenmyer flask at atmospheric pressure to boiling point. The sample was digested in less than 30 minutes. In 1980, the use of closed containers was introduced. Indeed, many researchers used this type of container for microwave digestion. This made it possible to reach temperatures higher than the boiling point of the acid mixture used, resulting in an increase in reaction speed and a decrease in reaction time. Later, Salgo and Ganzler developed the use of microwave ovens for the extraction of organic compounds from contaminated soil and plants [30]. However, the early techniques used did not meet all the needs that chemists were looking for at the time. In 1989, pressure control by feedback was introduced and three years later, temperature control, also by feedback, was introduced. After the implementation of these two techniques in sample digestions, the era of controlled digestions began.

Closed vessel digestion using microwaves is very common nowadays. This type of digestion allows the extraction of analytes from the sample with a significant reduction in the amount of solvent, digestion time, better efficiency compared to other methods and with less waste production. It is a method that is developing in the field of sustainable chemistry because it allows to protect the environment while achieving high performance. This method is therefore based on the use of microwaves, which refers to electromagnetic radiation with a wavelength of between 1 mm and 1 m in a frequency band ranging from 300MHz to 300 GHz [31]. This is a non-ionising energy range between the infrared and radio frequency regions of the electromagnetic

spectrum as shown in Figure 11.
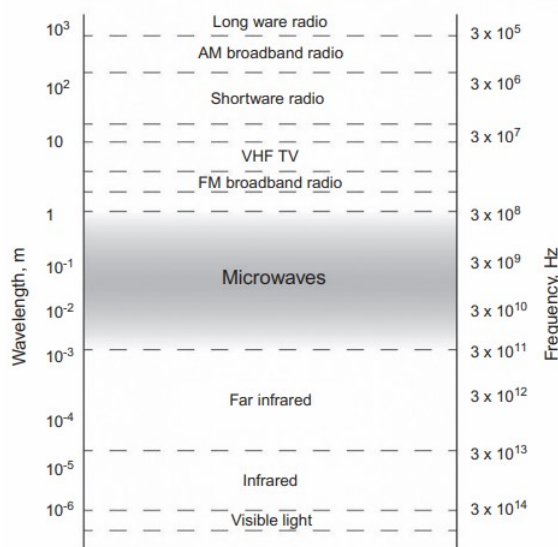
Figure 11: Range of electromagnetic radiation [31]

The method involves mixing the sample with a solvent mixture (usually acids) in a closed vessel and applying microwaves to the mixture. The solvents will then absorb the radiation from the microwaves and transform it into dielectric heating. This is because the polar molecules or ions in solution will absorb the microwave energy according to their ionic conduction and dipolar rotation. These molecules will begin to rotate many times per second and align themselves with the direction of the electric field. This will result in friction and collisions between the different molecules, which will generate a rise in temperature, an increase in pressure and a vaporisation of the liquid inside the vessels. The dipolar rotation therefore allows rapid heating of the mixture from both inside and outside, resulting in the absence of a thermal gradient. Compared to the open digestion method, there is an optimisation of the heat transfer resulting in a considerable reduction of the digestion time [31]. Figure 12 compares the temperature spread between the conventional heating method used in open digestion and the microwave heating method [32]. This figure shows that the sample is heated directly from the inside using microwaves and confirms the superiority of this technique over the open digestion method.
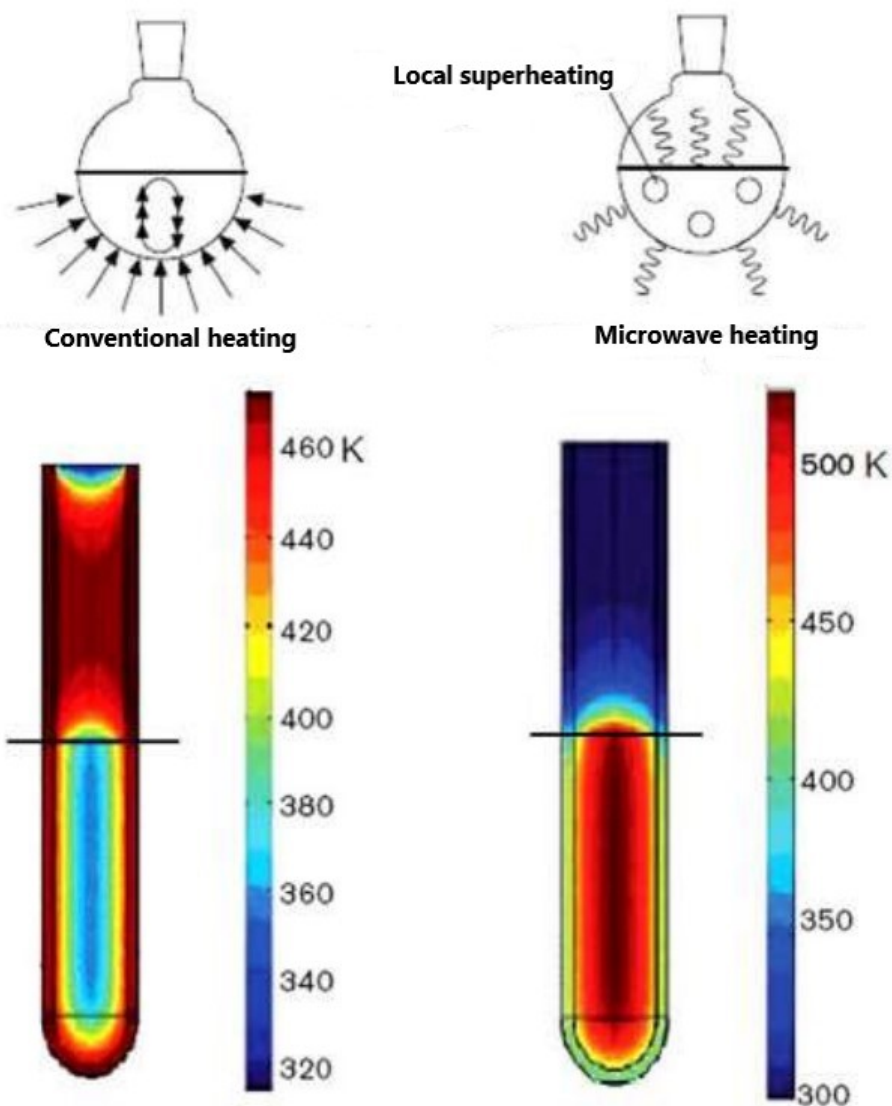
Figure 12: Temperature propagation according to the type of heating. With on the left: Open vessel digestion method. On the right: Closed vessel microwave digestion method [4]

It is important to use appropriate, selective and efficient solvents that will be able to solubilise the desired element such as polonium. A mixture of several different solvents with different dipole moments is usually used in order to obtain a better degradation of the organic or inorganic matrix [31].

Digestion by this method is carried out with a mixture of acids in a closed, microwave transparent, pressurised vessel to avoid contamination and loss of volatile elements. The microwave oven can perform the digestion for sample quantities up to 10 grams, with high concentrations of the element to be determined. In addition, the microwave oven allows control of both temperature and pressure, as well as power, all of which are time dependent. It should be noted that these parameters are programmed into the device according to the boiling points of the acid mixture or acid used. Compared to other conventional methods, this method has many advantages. It allows for higher recovery and efficiency of extractions while reducing energy and solvent consumption. It also reduces operating and service costs, as it does not require continuous monitoring by the analyst. This method will be the main one used in this work.

The experimental procedure for this method will be described later [33].

6.1.4   Procedures in the scientific literature

In the scientific literature, several digestion methods exist. For example, W. Flynn proposes to carry out an open type digestion for soil samples. Their method consists of adding 10 ml of concentrated nitric acid and 10 ml of 70% perchloric acid to an aliquot of the sample. Then he evaporates until white smoke appears and dries the mixture using infrared heating at 120°C. After drying, 5 ml of chloridric acid is added to the aliquot and heated until the dry residue is dissolved. The whole is then transferred to a 150 ml beaker. A final rinse is carried out by adding 5 ml of boiling chloridric acid [33].

On the other hand, Guogang propose a combined melt digestion and open digestion method for the pre-treatment of soil and rock samples. A first treatment is performed by taking 1g of the sample which is then mixed with 2g of Na_2CO_3 and 2g of Na_2O_2 (fluxer). The whole set is placed in a 30 ml platinum crucible and mixed. The crucible was then placed in a muffle furnace at 600°C for 10 minutes. Once cooled to room temperature the digestion can begin. The first step is to transfer the contents of the crucible into a 100 ml Teflon beaker and add 15-20 ml of concentrated nitric acid and water. Then 5 ml of concentrated nitric acid, chloridric acid and 40% hydrofluoric acid are added to the beaker. The whole is evaporated at 200-250 °C and the operation must be repeated 2-3 times. Then 20 ml of 72% $HClO_4$ is added and evaporated. Then two 5 ml portions of concentrated HCl are added consecutively to change the medium of the solution and evaporated to dryness. The residue is finally dissolved with 35 ml of 6 M HCl [29].

For plant samples, M.L. Jackson proposes to use an open digestion using an acid mixture of 100 ml nitric acid, 10 ml sulphuric acid and 40 ml 60% perchloric acid for 2g of dried sample. This is then digested at 180-200 °C until dense white fumes of H_2SO_4 and $HClO_4$ are produced. The digestion continues until the acidic liquids are barely volatilized. If during the operation the acidic liquid turns brown, 5 ml of the acid mixture is added and the digestion is continued as before. When the residue is white and clear, the digestion can be stopped [34].

6.2   Separation methods for polonium

The aim of the separation is to extract the Po-210 (and its tracer) from the sample after digestion. The Figure 13 shows the main separation routes found in the different scientific papers. The main separation techniques are:

- Solvent extraction

- Chromatography

- Spontaneous deposition

Solvent extraction is the use of a chemical extraction solvent such as isopropyl ether, methyl isobutyl ketone (MIBK), diisopropyl ketone, and tributyl phosphate to separate a substance in a solid phase. This solvent is very effective in extracting Po-210 in acidic solution. It is generally used in the purification of Pb-210 containing solutions by removing the Po-210. However, in this work, all the samples will be solubilised. Therefore, solvent extraction becomes unnecessary in this case [35].

In terms of chromatographic methods, anion exchange chromatography has often been applied as a separation or purification method. Some resins, such as Bio-Rad AG1-X4 resin, have proven to be effective in separating Po-210 and Pb-210 in acidic media [35]. Guogang use it to separate Pb-210 from their sample [29]. This shows that chromatography is a technique often used for the purpose of separating Pb-210 and Po-210.

Spontaneous deposition remains the optimal choice for measuring Po-210 in natural samples. Indeed, deposition allows the direct isolation of Po-210, is less expensive and easier to set up. For all these reasons, spontaneous deposition was chosen.
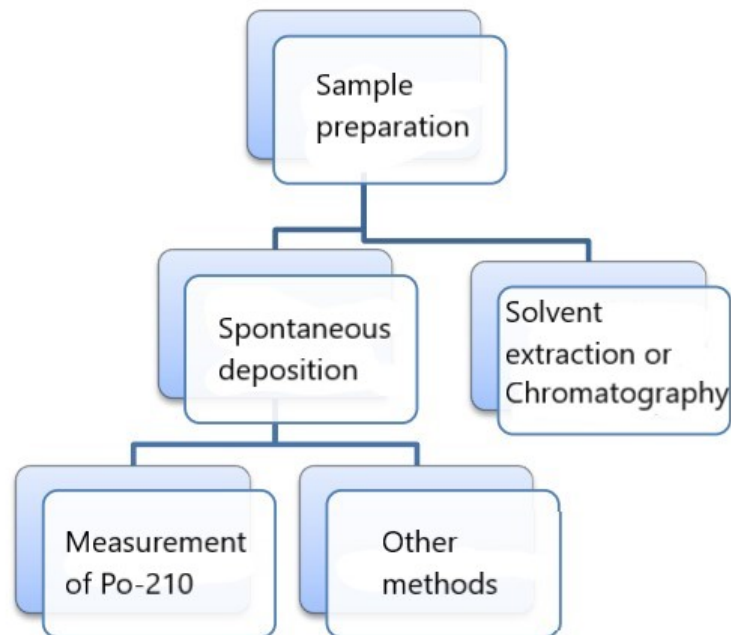
Figure 13: Diagram of the analysis procedure for Po-210

6.2.1 Deposition

The separation procedure consists of a spontaneous deposition of the Po present in solution on a silver plate. The deposition results in a thin, uniform layer of high resolution on the surfaces of metal discs such as silver, copper, nickel and stainless steel discs [35]. Silver plates were chosen because of their high efficiency compared to other types of plates (Figure 14)

Disque	rendement de dépôt (%)
Argent	90
Nickel	82
acier inoxydable	83
Cuivre	83

Figure 14: The deposition efficiency of each disc cite [35]

The spontaneous deposition process requires a rigorous protocol to be followed in order to maximise its efficiency. The deposition on the disc must be as fine, uniform and stable as possible in order to allow the alpha particles to pass through during the measurement.

The method proposed by W.Flynn for Po deposition uses 5 ml of Hydroxylamine Hydrochloride 20%, 2 ml of Sodium citrate 25% and 10 mg of Bi carrier. The pH of the solution is then adjusted to 1,5 using ammonia (NH_3). Distilled water is then used to dilute the solution to 50 ml. The solution, placed in a Teflon beaker, is heated to 85-90 °C and stirred with a stirrer until the yellow colour disappears. After removing any air bubbles present, a silver plate is then placed in the Teflon beaker containing the solution. The solution is then stirred with the stirrer for 1 hours and half at 85-90°C. Once the time is up, the silver plate is washed with demineralised water and methanol. The plate is then dried and ready for spectrometry [33]. The method proposed by Guogang is very similar. The only difference is the concentration of Sodium citrate how is 25% and the time of deposition (4 hours).

7 Polonium detection

There are two main ways to measure alpha decay from polonium-210. The first is to use alpha spectrometry. Alpha spectrometry consists of using a Silicon detector belonging to the semiconductor family. The second way is to use liquid scintillation which allows the detection of alpha and beta minus radiation.

7.1 Alpha spectrometer: Principle of the Silicon detector

The Silicon (Si) detector is a member of the family of semiconductor detectors. They are composed of a crystalline solid medium placed between 2 electrodes. When ionising radiation passes through the detector, e^-/hole (h^+) pairs are created. An electric field will then collect these pairs. Generally, the use of this type of detector requires a low temperature (like the Germanium detector) but this is not the case for the Silicon detector.

Semiconductor detectors are made up of three zones (see Figure 15).

- The conduction band : Band containing free e^-.

- Valence band : Band containing e^- bound to atoms.

- Gap band: A region of forbidden energy.

These energy bands are made up of several closely spaced electronic states called continua. The valence band and the conduction band are separated by a gap $\Delta E \approx 1eV$ corresponding to the band of forbidden energy domains.
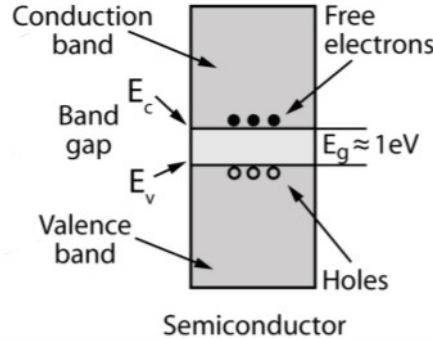
Figure 15: Semi-conductor [36]

When the temperature is 0 K, the conduction band is empty because all e^- are still connected to their atom in the valence band. There will therefore be no current if an electric field is applied. At room temperature, a number of e^- in the valence band will be excited to the conduction band due to thermal fluctuations. This will result in a hole (h^+) at the original position of the excited e^- in the valence band and make the conduction band carry a negative charge. Then one of the e^- further into the valence band can fill a h^+ present near the gap band. This mechanism is capable of repeating itself in such a way that it results in the movement of h^+ positive charge carriers through the crystal. Therefore, the application of an electric field produces a current. It is therefore possible to have a current due to the movement of free e^- and h^+ in the valence band in a semiconductor [36].

In the case of the Si detector, a PN junction is used. This consists of the combination of a P-doped semiconductor and an N-doped semiconductor.

In the case of an N-doped semiconductor, a pentavalent impurity (doping) such as phosphorus (e^- donor element) is introduced into the Si which is tetravalent. There is thus a replacement of an atom of Si by an atom of Phosphorus (P). This leads to the appearance of an additional e^- weakly bound and therefore easily excited towards the conduction band. The energy of this localised level will be some 10^{-2} eV below (Figure 16) the conduction band. There is therefore an e^- in the conduction band without there being an h^+ in the valence band [36].

In the case of a P-doped semiconductor, it is a trivalent impurity that is introduced such as boron (e^- accepting element). A replacement of an atom of Si is thus operated, resulting in an additional h^+ since there is not enough e^-. Therefore, an e^- that will be captured in this h^+ will be less bound and thus the energy level will be located just above (Figure 16) the valence band top. There is thus an additional hole in the valence band without e^- in the conduction band [36].
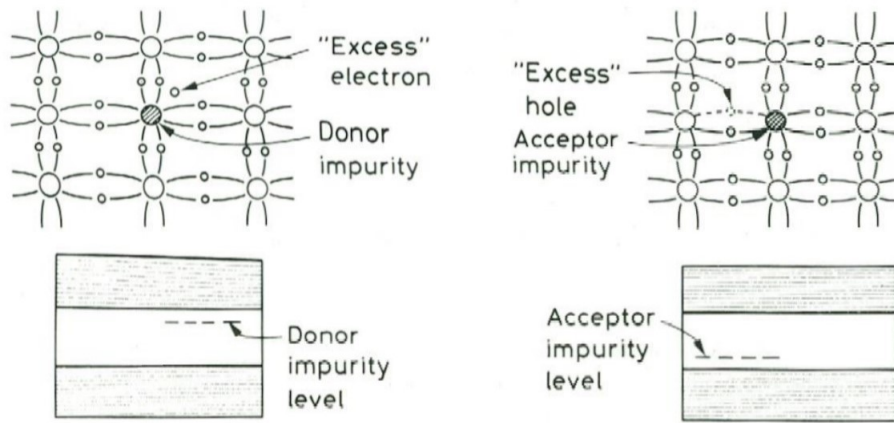
Figure 16: Representation of doped semiconductors with N-doped semiconductor on the left and P-doped semiconductor on the right [36]

At the junction of the two doped semiconductors, a recombination of e^- and h^+ takes place. This area is called the depletion zone. If an external voltage is applied such that the anode is at a negative potential relative to the cathode (reverse biased), the h^+ in the p-region and the e^- in the n-region will be drawn away from the junction causing an increase in the depletion zone which will restrict the current flow. Thus, when radiation (in this case alpha radiation) passes through the depletion zone of the detector in reverse polarisation, many e^- - h^+ pairs are created. Then a migration of e^- to the positive pole and h^+ to the negative pole takes place. The number of pairs is proportional to the energy deposited by the radiation in the p-n junction and therefore the voltage pulse across a resistor will be proportional to the energy deposited by the radiation allowing spectrometry and counting. The diagram in the Figure 17 shows the complete counting chain for alpha spectrometry. The e^- produced when the alpha radiation interacts with the detector will first be amplified before being displayed as an energy spectrum using an ADC (analogue-to-digital converter) and a MCA (multi-channel analyser).
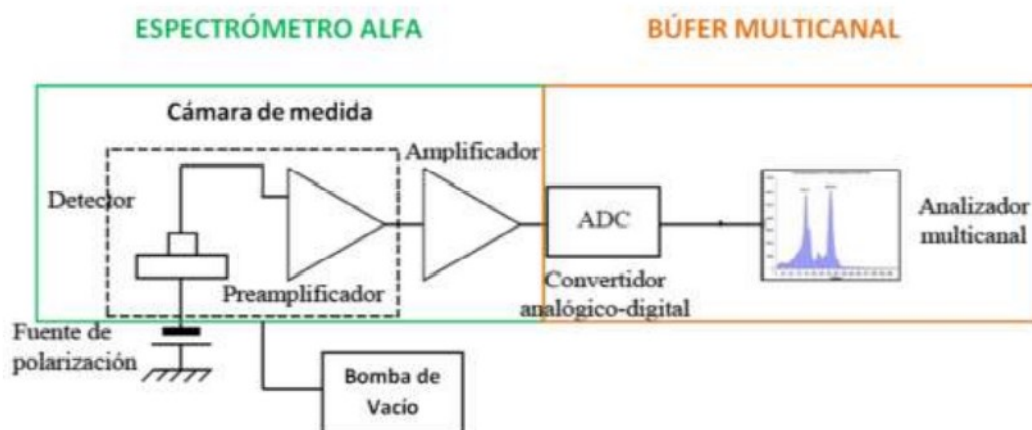
Figure 17:   Block diagram of an alpha spectrometer

As mentioned above, the Si detector is used at room temperature and has an average energy for the creation of an e^- - h^+ pair of 3.62 eV. On the other hand, the relatively small size of the depletion zone makes it useless for charged particles with a large mean free path,

such as gammas. That said, it is perfectly suited to the study of alpha decays given their small mean path [36]

7.2   Liquid scintillation

Another method of detection is to use liquid scintillation. This technique is used for the measurement of β^- and α ionising radiation. It was developed by Kallman and Reynolds in the 1950s. This technique consists of using a scintillating cocktail containing one or two fluorescent substances that can be excited indirectly by the particles emitted by the sample. This technique is therefore based on the interaction between the emitted particle and matter. When a particle interacts with the scintillating cocktail, electromagnetic radiation is created. In addition, an energy transfer cascade takes place between the fluorescent molecules. This energy transfer cascade increases the wavelength of the electromagnetic radiation (photon) to a level detectable by a photomultiplier. The Figure 18 shows the general principle of this method. In effect, the radionuclide emits α or β^- ionising particles which can excite the solvent molecules. This excitation is then transmitted by the fluorescent molecules (energy transfer cascade). After a certain time, these molecules de-excite by emitting a photon in the visible range that can be detected by a photomultiplier. The number of photons emitted is proportional to the energy absorbed by the scintillator and the number of nuclei that decay. The photomultiplier will allow it to create a large number of e^- in proportion to the energy of the emitted photon. The photomultiplier will allow to obtain an electric signal, which completed with an electric system, allows to obtain a spectrum [17]
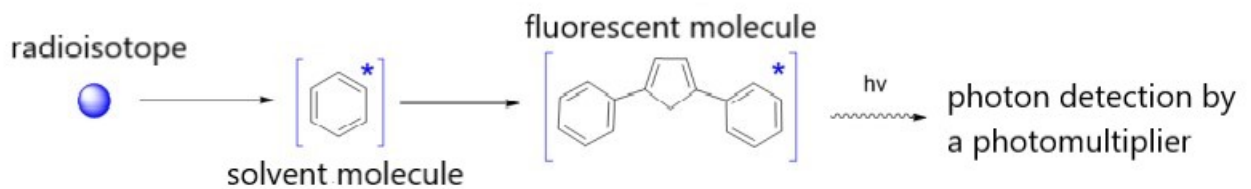
Figure 18:   Diagram of the excitation of scintillating molecules by ionising radiation [17]

The main advantages of this technique are the ease of preparing the sources for measurement, the detection efficiency of 4π and the absence of a physical barrier between the radionuclide to be measured and the detector. It allows the quantification of low energy radiation [17]. Unfortunately, this technique also has its shortcomings. The first is related to physico-chemical phenomena that reduce the efficiency of the scintillator, known as quenching. Quenching causes a shift in the spectrum towards low energies as shown in Figure 19. There are two types of quenching. The first is chemical quenching. It is caused by the disturbance due to the excitation of the solvent molecules [37]. The second is optical quenching. It is caused by the loss in photon energy transfer due to the opacification or colouring of the solution [37]
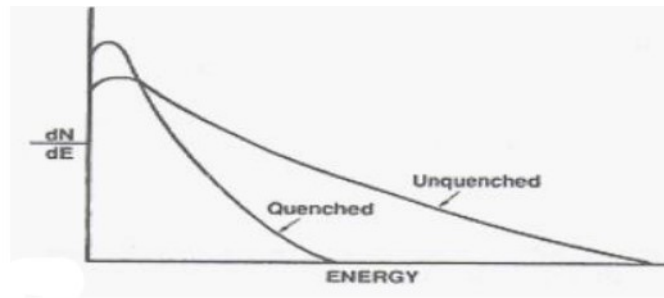
Figure 19: Quenching effect [37]

In addition, this technique becomes more complex to use for Po-210 spectrometry. Indeed, when measuring Po-210, a tracer such as Po-209 is used in order to be able to calculate the chemical recovery of the method used when preparing the measurement sample. The resolution of the liquid scintillator is very high. The two peaks are therefore superimposed and cannot be distinguished. The Figure 20 shows this superimposition of peaks. The figure shows that the Po-209 peak (4,88 MeV [9]) is superimposed on the Am-241 peak (5,50 MeV [9]). However, the energy of Po-210 (5,30 MeV [9]) is between these two energies. Therefore, the Po-210 peak is confused with the Po-209 peak. It therefore becomes difficult to calculate the chemical recovery of the method under these conditions. The choice of the measurement method will therefore be more in the direction of alpha spectrometry.
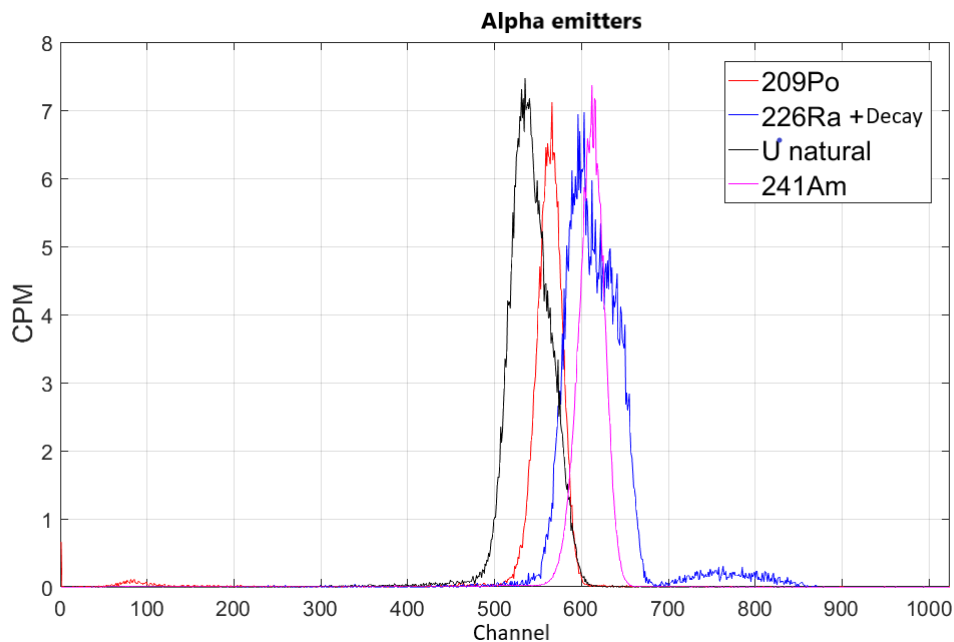
Figure 20: Superposition peaks with the liquid scintillation technique [38]

Chapter 2: Experimental part

1 Introduction

The experimental part consists in finding an efficient way to quantify Po-210 in natural samples such as soils, plants and aerosols. For this purpose a series of steps are necessary in order to measure Po-210. In general, the main steps are the following:

- Pre-treatment, which consists of drying, digesting, evaporating and filtering the different samples

- Separation of the analyte, which consists of isolating the Polonium

- Alpha spectrometry to quantify the polonium present in the samples

Generally, the last two steps are very similar according to the scientific literature. The only point of divergence concerns the pre-treatment. There are a number of procedures for the pre-treatment of natural samples in the literature depending on the type of sample and the type of equipment available and usable. It is important to emphasise the importance of pre-treatment. Indeed, the choice of the digestion method is essential in order to avoid as much volatile loss of Po-210 as possible. The study will focus on different types of natural organic and inorganic samples as shown in the following Table 2:

Table 2: Samples information

Name	Types	Category	Origin
MI 38	Soil	Inter-comparison	IAEA
MI 67	Soil	Inter-comparison	IAEA
FV	Glass fiber filter (aerosols)	Natural	Air pumps UPV
FC	Cellulose filter (aerosols)	Natural	Air pumps UPV
TA	Tobacco	Natural	Commercial tabaco
PL Grass/plant	Grass	Natural	Front of building 5i (UPV)
Gilet	Soil	Natural	Soil UPV

The complete methodology is resumed in the appendix A

2 Description of the samples

This section will describe the set of samples used in this work. Some of these samples are inter-comparison samples to compare the values obtained experimentally with those given by the IAEA. The other samples are of natural types, mainly from the UPV and other locations.

2.1 Inter-comparison samples

The inter-comparison samples are very useful as they allow to see the accuracy of the method. These samples come from the IAEA (International Atomic Energy Agency) and are composed of several alpha, beta and gamma emitters including Po-210 or Pb-210. The objective will therefore be to compare the measurements given by the IAEA and the results obtained by the method used in this work.

2.1.1 Soil MI38

The sample MI38 is a soil sample collected in 2012 in Jeju Island, Republic of Korea (Figure21). This sample contains several types of natural and anthropogenic radioisotopes such as Po-210. This sample was supply the IAEA in the proficiency test IAEA-TEL-2012-03. According to the reference document in the appendix B, the specific activity of Po-210 on 01/01/2012[3] is $573 \pm 25 Bq/kg$ and $595 \pm 19 Bq/kg$ for Pb210 [4] [39]. Taking into account the uncertainties, these two elements are in secular equilibrium in the sample. A calculation is therefore necessary to determine the specific activity in 2022. Assuming that Pb-210 [5] decays directly into Po-210. Secular equilibrium means that the activity of Pb-210 and Po-210 are identical. The calculation of the specific activity of Po-210 in 2022 can therefore be done directly from Pb-210. Equation 16 gives the specific activity of Po-210 on 26/05/2022.

$$A_{MI38} = A_0 \cdot e^{-\lambda t} = 430,67 Bq/kg \tag{16}$$

With :

- A_{MI38}: Po-210 activity on 26/05/22 [Bq/kg]

- A_0: Pb-210 activity at the reference date (01/01/2012) = 595 Bq/kg

- λ: The decay constant of Pb-210 = $8,51 \cdot 10^{-5} \ s^{-1}$

- t: The time in days between the reference date and the date of 26/05/2022 = 3798 days

The specific activity value of Po-210 at the time of the measurements is $430,67 \pm 13,75 Bq/kg$. The aim will be to compare this value with the measurements made in the laboratory at LRA.
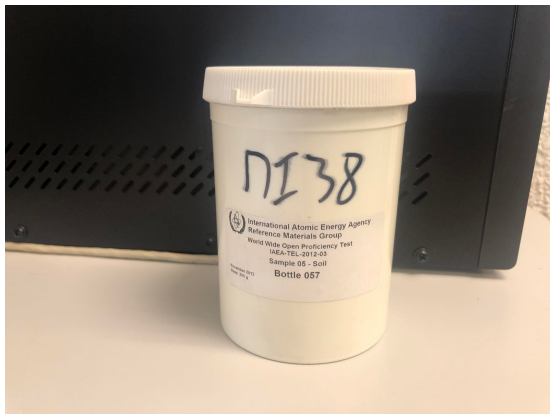
Figure 21: MI38 sample from IAEA

---

[3] All the date in this document are given in dd/mm/yyyy

[4] All the uncertainty in this work is taken for k=2

[5] This supposition is possible because the half-life of Bi-210 (5 days) which is the element between Pb-210 and Po-210 in the decay chain, is negligible compared to the half-lives of Pb-210 (22,3 years) and Po-210 (138 days)[9]

2.1.2 Soil MI67

Sample MI67 is also a soil sample (Figure 22). It was collected in 2018 in Hungary by the Food and Feed Safety directorate. This sample also contains radionuclides such as Pb-210 and Po-210. This sample was supply by the IAEA in the proficiency test IAEA-TEL-2018-03. According to the reference document, which can be found in the appendix C, the specific activity in Pb-210 on 01/01/2018 is $485, 0 \pm 11, 6 Bq/kg$ [40]. However, no value is given for Po-210. We can make the supposition (verification of this supposition will be done in the results section) that it is in secular equilibrium with Pb-210 and therefore has the same activity. The equation 17 therefore allows us to calculate the activity of Po-210 on 26/05/2022.

$$A_{MI67} = A_0 \cdot e^{-\lambda t} = 423, 04 Bq/kg \tag{17}$$

With :

- A_{MI67}: Po-210 activity on 26/05/22 [Bq/kg]

- A_0: Pb-210 activity at the reference date (01/01/2018) = 485 Kg/Bq

- λ: The decay constant of Pb-210 = $8, 51 \cdot 10^{-5} \ s^{-1}$

- t: The time in days between the reference date and the date of 26/05/2022 = 1606 days

The specific activity value of Po-210 at the time of the measurements is $423, 04 \pm 10, 12 Bq/kg$. The aim will be to compare this value with the measurements made in the laboratory at LRA.

Figure 22: MI67 sample from IAEA

2.2 Natural samples

The natural samples are described here. The amount of Po-210 present in them will be much lower than in the intercomparison samples. The samples studied are tobacco, aerosols, grass and a soil sample.

2.2.1 Aerosols

The study of Po-210 in aerosols is carried out using two types of filters placed in two different pumps. The two pumps (Figure 23) will suck the aerosols present in the air around them with a variable flow rate between 30 and 50 L/min. The filters will trap these aerosols.

Figure 23: Pump n°1 on the left. Pump n°2 on the right

Two types of filters were used . The first is a glass microfiber filter (FV) (Figure 24).

Figure 24: Glass Microfibre filter

The second filter is a cellulose filter (FC) (Figure 25).

Figure 25: Cellulose filter

Four filters of FC and three of FV were placed in the pumps between the end of 2021 and the beginning of 2022. The Table 3 shows all the information about these filters. Unlike the other samples, the specific activity measured on the filters will be given in Bq/m^3. Two blank filters were also analysed (one of each type).

Table 3: Filters Samples information

Sample n°	Date begin	Date end	Volume of air [m^3]	pump n°
1 (FV)	22/12/2021	29/12/2021	414,03	1
2 (FV)	22/12/2021	29/12/2022	490,00	2
3 (FV)	29/12/2021	05/01/2022	412,92	1
4 (FC)	05/01/2022	12/01/2022	342,01	1
5 (FC)	05/01/2022	12/01/2022	431,39	2
6 (FC)	12/01/2022	19/01/2022	336,49	1
7 (FC)	12/01/2022	19/01/2022	434,30	2

2.2.2 Tobacco

The study of Po-210 in tobacco is very important. Indeed, tobacco can contain significant concentrations of Po-210 due to the use of apatite-based fertilisers [35]. This Po-210 comes mainly from atmospheric fallout and resuspension of Po-210 from the soil. The cumulative alpha radiation dose due to the radioactive content of inhaled cigarette smoke and the increasing number of lung cancer cases explain the interest in measuring Po-210 in tobacco.The smoke inhaled by smokers contains a little proportion of Po-210 but is already potentially dangerous, of the order of 5 to 10 µSv per cigarette [35]. The tobacco analysed in this work is the "Ideales Picadura Selecta" brand of rolling tobacco from the Figure 26.
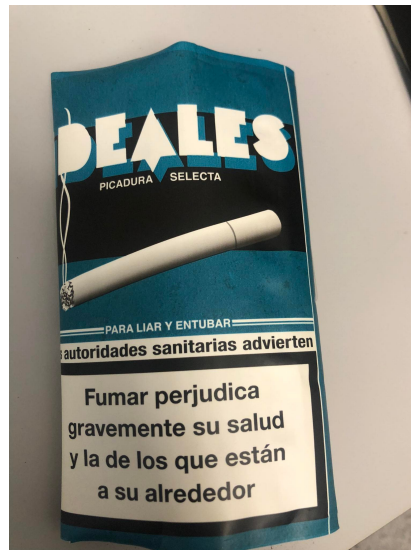
Figure 26: Rolling tobacco: "Ideales Picadura Selecta"

2.2.3 Grass

The grass samples were collected from the lawn in front of the UPV building 5i on 07/04/2022 (Figure 27). The amount of Po-210 is expected to be very low or even below the detection limit. If Po-210 is present in this sample, its origin may be mainly from atmospheric fallout and resuspension of Po-210 from the soil. It is also maybe due to the fertilizers used in the soil.
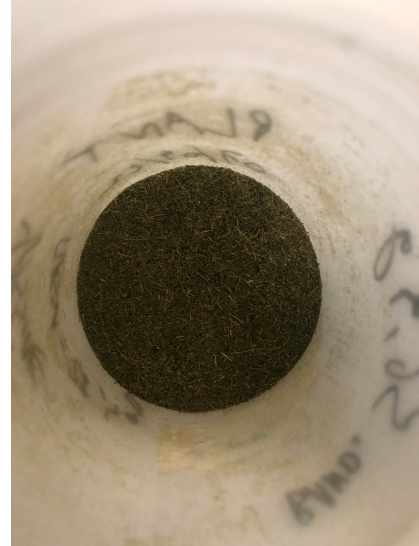
Figure 27: Grass sample from the lawn in front of the UPV bulilding 5i

2.2.4 Soil Gilet

This soil sample was collected from Gilet, a town north of Valencia (Figure 28) on 02/04/2021.

Figure 28: Localisation of Gilet on a map

This sample was taken in a forest located in Gilet (Figure 29). This sample was taken in order to verify its possible contamination by Po-210.
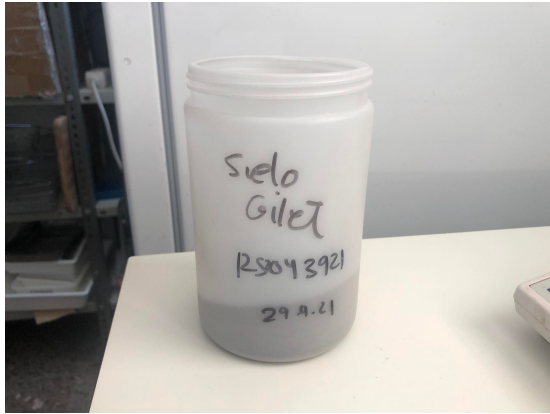
Figure 29: Soil sample from a forest of Gilet

3 Pre-treatment of samples

Sample pre-treatment is an extremely important step in the process. The main objective of this step is to dissolve as much of the polonium present in the sample as possible with the least amount of loss. Indeed, polonium is quite volatile making the risk of loss quite high. It is therefore essential to pay attention to the heating temperature during the various stages. According to Flynn, from 150°C onwards, polonium becomes volatile, leading to losses, so it is important never to exceed 120°C during drying and evaporation or other heating process [33]. As mentioned above, the pre-treatment of the different samples is divided into 4 main steps:

1. Drying

2. Digestion

3. Evaporation

4. Filtering

All these steps were applied to the different types of samples mentioned in the previous section.

3.1 Drying

Drying is carried out with the aim of removing as much water as possible from the samples. Drying was carried out using the laboratory oven shown in Figure 30. The drying process is quite simple. All samples, except the air filters, were dried at a temperature of 80°C for about 12 hours. Once the samples were dried, only the plant samples were sieved in order to obtain a sample as homogeneous as possible. The air filters were just cut into six pieces and placed directly into the vessels for digestion.
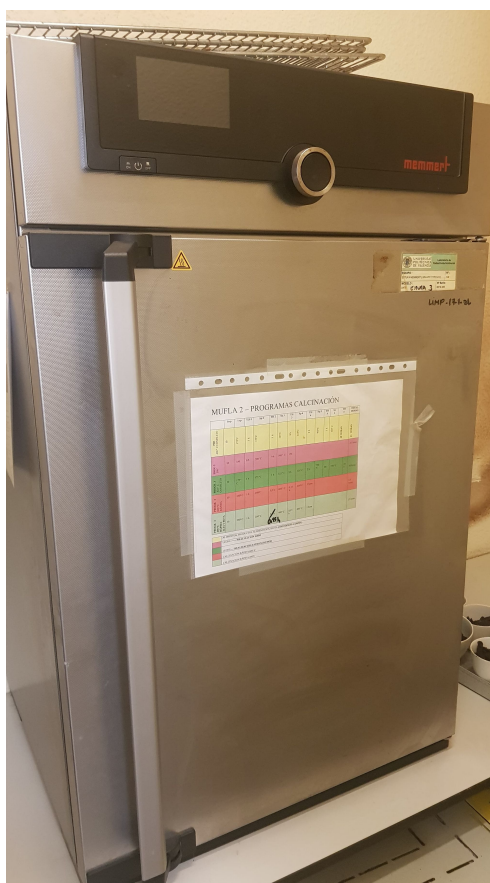
Figure 30: Drying oven from the LRA at UPV

3.2 Digestion

Digestion is one of the most complicated steps to implement. Indeed, there are many different digestion methods depending on the type of sample. The different methods proposed are quite interesting. However, some of them contain certain defects such as the heating temperature often exceeding 120°C or the missing material. The objective of this work was to find a digestion method that could be generalised to all samples, regardless of their type, and the choice was made to use a closed vessel microwave digestion method often used in the UPV laboratory. This method will therefore be described, but first it is important to describe the equipment used in this method. This is the Multiwave Go microwave from Anton Paar.

3.2.1 Microwave Multiwave Go

The microwave digestion system used in this work is called the Multiwave Go and is shown in Figure 31. This system is optimised for the analysis of environmental samples, plant material, food quality control and other materials. The system is very cost effective as it requires very little solvent and is commonly used in routine analysis.

Figure 31: Microwave Multiwave Go from the LRA at UPV [41]

The Mutliwave go has a corrosion resistant aluminium rotor. It can acquire up to 12 teflon vessels of 50 ml each and delivers up to 850 W of power. In addition, the Multiwave Go is characterised by a short digestion process that can achieve a digestion rate of 12 samples in 18 minutes. This makes the Multiwave Go one of the fastest digestion device on the market with the widest heating range. In addition to its light weight, it is equipped with a sensor system for monitoring the rotor revolution and temperature, which is very useful in case of sample overheating. It can reach a temperature of 250°C and a pressure of 20 bars [41]. It has a cooling system that allows the continuous removal of the heat produced during the reaction. A ventilation system also allows the overpressure of the gases to be extracted thanks to a new ventilation concept that is activated in the event of too high a pressure. Once the reaction process is complete, the vessels are automatically cooled and depressurised. An IR temperature sensor provides strict control of the reaction in case of overheating. Indeed, the IR sensor, shown in the Figure 32, allows the magnetron to be switched off immediately. It is therefore important to check this sensor frequently and to adjust it by performing a temperature calibration [41].
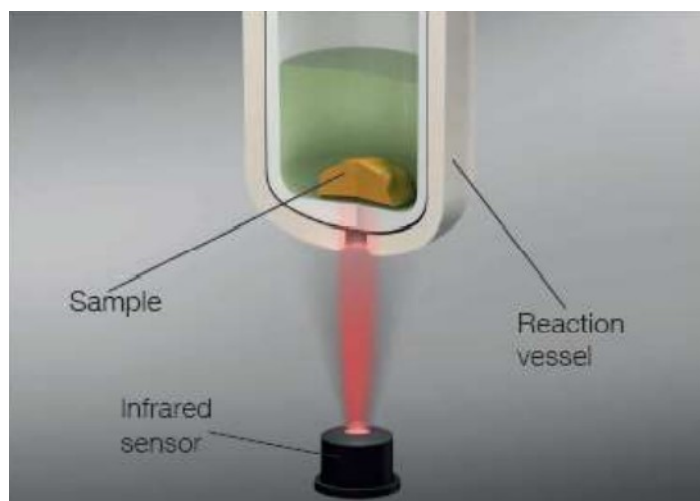
Figure 32: Infrared sensor for temperature control [41]

3.2.2   Temperature calibration

Before starting any digestion, it is essential to perform a temperature calibration of the IR sensor. Indeed, it is the sensor that allows, in case of overheating problem, to stop the process.

If the sensor is incorrectly calibrated, this can lead to extremely dangerous losses of samples and acids that can damage the machine or, worse, affect the operator. The company selling the Mutliwave Go recommends that this calibration is carried out once a month. In case strange temperatures are detected after a digestion, the IR sensor must be rechecked and therefore recalibrated. The Figure 33 shows the different steps required for calibration. The first step is to open the machine and remove the drive ring. Then you have to place the calibration unit in the holes and connect it as shown in the Figure 33 (C, D, E). The calibration unit will give the temperature in the machine and compare it to the temperature given by the IR sensor. Once all these steps have been completed, the calibration process is started [41].
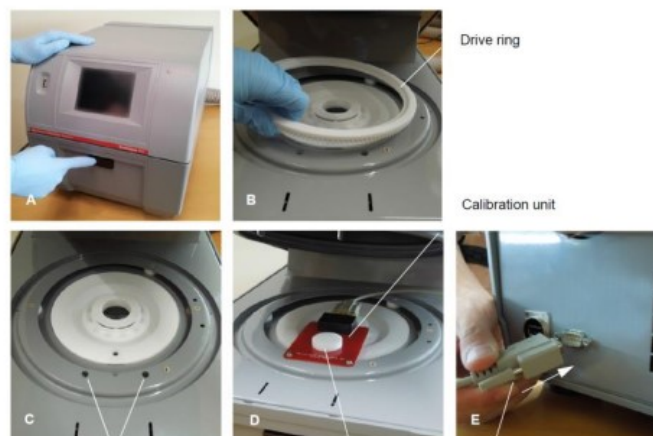
Figure 33: Placing of the Calibration Unit in the equipment for IR sensor calibration [41]

Once the calibration has been completed, a table with the results is provided by the machine. The table shows the values obtained during one of the calibrations carried out during the work. For the calibration to be considered valid, the values obtained by the unit calibration must be similar to the temperature values obtained by the IR sensor, allowing a range of $\pm 5^{\text{o}}$C [41].

Table 4: Temperature calibration table

Setpoint ($^{\text{o}}$C)	IR Sensor ($^{\text{o}}$C)	Calibrator ($^{\text{o}}$C)
40	39,2	40
50	49	50
75	73,5	75
100	98	100
130	127,5	130
150	147,3	150
170	167,1	170

3.2.3 Functioning and Methodology

The Mutliwave Go is used to destroy organic and inorganic sample matrices using highly concentrated acids. Proper digestion allows the analytes of interest to be brought into solution for subsequent measurement by various methods. The system has two processes, acid digestion and acid leaching. Acid leaching is used to determine the amount of leached elements and is

not used in this work. However, acid digestion will be very useful as it leads to the total or partial destruction of the matrix. During acid digestion, certain acids are used and are listed below:

- Nitric acid, HNO_3 (65%)

- Hydrochloric acid, HCl (30-32%)

- Hydrogen peroxide, H_2O_2 (30

- Hydrofluoric acid, HF (40-48%)

- Boric acid, H_3BO_3 (cold saturated solution, 5-5.5%)

- Sulphuric acid, H_2SO_4 (96%) (with restrictions)

- Phosphoric acid, H_2PO_4 (85%) (with restrictions on use)

In this list, only nitric acid, hydrochloric acid, hydrogen peroxide and hydrofluoric acid are used. These are the main acids used in the various digestions. Hydrofluoric acid, which is extremely dangerous, is very useful for more complex matrices containing Si and Al. In addition, Multiwave Go comes with the facility for several methods for direct use. The table in Figure 34 shows the information for each method [41].

Nombre del método	Tipo de aplicación	Modo recipiente	T-Límite (ºC)	Tª modo control	Mezcla de ácidos	Programa rampa(min)/Tª(ºC)/tiempo(min)
Cleaning	Digestión	MV*	200	Promedio	8-15mL mezcla ácido con HNO₃ y/o HCl y/o H20	10:00/180/05:00
EPA 3015A***	Digestión				2,5mL HNO₃ o 2mL HNO₃ + 0,5mLHCl	10:00/170/10:00
EPA 3015A**	Digestión				10mL HNO3 o 9mL HNO3 + 3mL HCl	05:30/175/04:30
EPA 3052	Lixiviación				HNO3/HF/HCl/H2O2	10:00/180/09:30
Inorganic	Digestión				8-12 mL Agua regia	10:00/165/10:00
Organic A	Lixiviación				6-10 mL HNO3 + 0-2 mL HCl + 0-1 mL H2O2	20:00/180/10:00
Organic B	Digestión			Máximo	6-10 mL HNO3 + 0-2 mL HCl + 0-1 mL H2O2	10:00/100/10:00 10:00/180/10:00
PQ***	Digestión				9,9 mL H2O + 0,1 mL HNO3	01:00/180/10:00

***media escala   MV*: modo multivessel

Figure 34: Pre-installed methods in Multiwave Go [41]

The method used in this work is a combination of a slightly modified version of the Organic B method and an added method called HF. The Organic B method was modified by the LRA staff and is called Organic B_LRA. The Table 5 shows the characteristics of the two methods used for the digestion of the samples.

Table 5: Organic B-LRA and HF methodology [41]

Methods	Recipe	n°	Ramp [mm:ss]	Temperature [°C]	Hold [mm:ss]
Organic B-LRA	8ml HNO_3	1	15:00	100	04:00
	+ 2 ml HCl	2	15:00	165	08:00
	+ 2ml H_2O_2				
HF	2 ml HF	1	10:00	150	05:00

As shown in the table, the first step is to place an aliquot of the dried sample in the vessels and first add the 8 ml of HNO_3 and the 2 ml of HCl. However, the addition of H_2O_2 must be done very carefully. Indeed, the addition of H_2O_2 will cause an effervescence of the sample which can lead to a loss of sample and acid in case of rapid addition as shown in the Figure 35. This effervescence will be all the stronger if the sample is very organic. The solution is to first add 1 ml of H_2O_2 per small drop. After 15-30 minutes, the last 1 ml is also added per drop.

Figure 35: Effervescence reaction because of H_2O_2

Once this is done, each vessel is closed to avoid any loss during digestion. The Figure 36 shows how the vessels are closed.
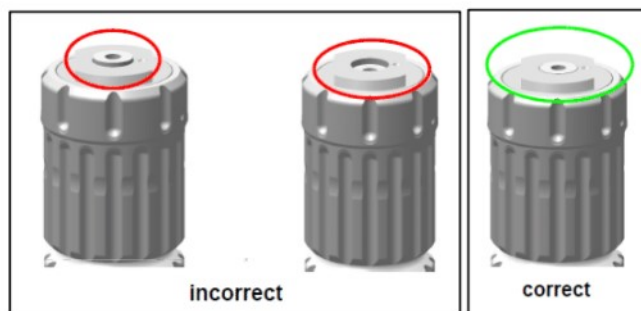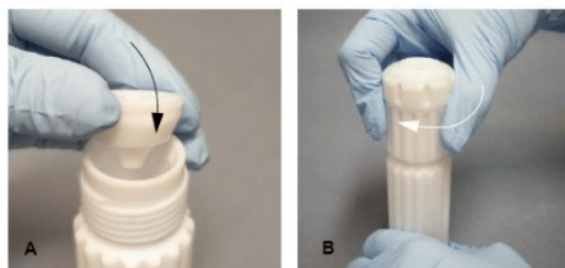
Figure 36:   Correct and incorrect positions of the screw cap on the vial [41]

Once closed, the vessels should be positioned symmetrically according to their number as shown in the Figure 37. This will ensure a uniform temperature in all vessels during digestion. For the sake of efficiency, it was decided not to exceed 6 vessels per digestion to ensure optimal digestion. If only one vessel is used, this must be indicated on the instrument by means of the "single vessel mode" function.
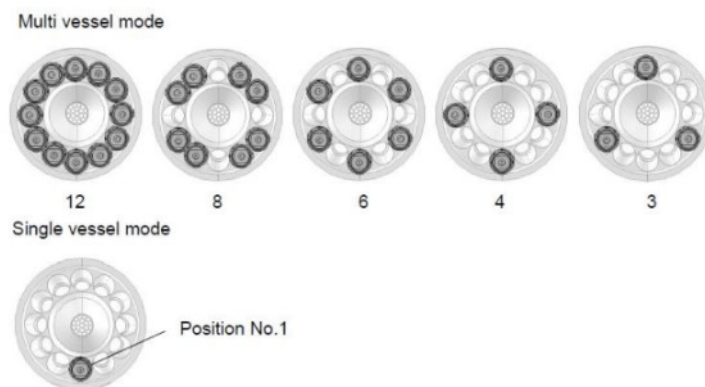
Figure 37:   Correct positioning of the vials in the rotor [41]

Once the vessels have been placed in the structure, a lid is placed on the vessel and placed on the drive ring of the machine as shown in the Figure 38. The machine is then closed. For safety reasons, it is also important to put a vent tube in a fume hood in order to evacuate the various acid vapours. Once all these steps have been completed, the Organic B_LRA program is started.
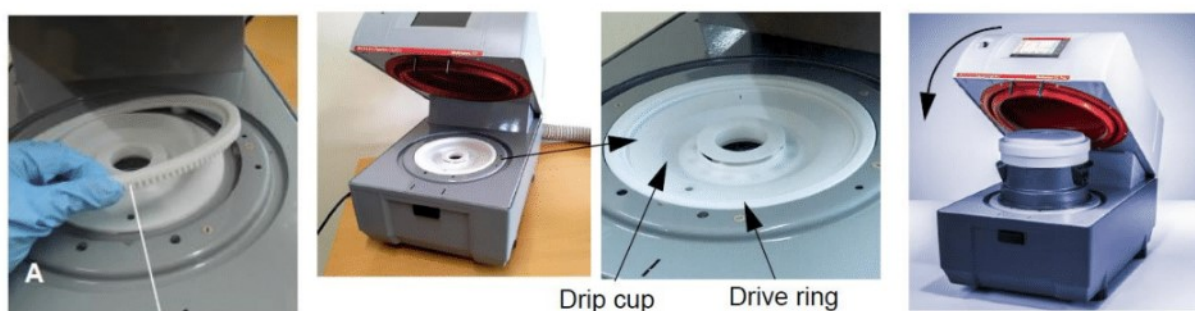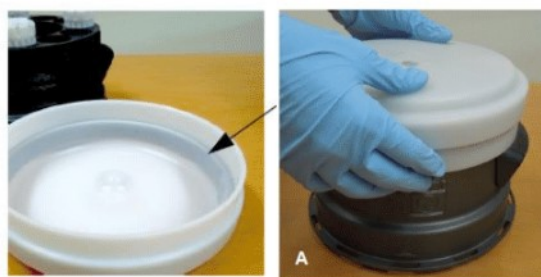
Figure 38: Correct positioning of the vials in the rotor [41]

After the Organic B_LRA digestion is completed, a graph of the temperature evolution (and the power (p)) during the digestion as a function of time is provided by the Multiwave Go system and is shown in Figure 39 . The vessels are then opened and 2 ml of HF is introduced. The vessels are then closed and placed back into the machine in the same way as before.
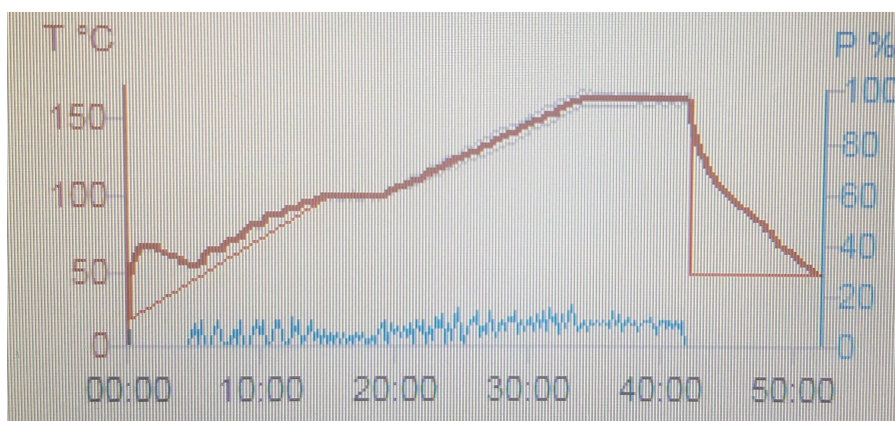
Figure 39: Graph of the temperature evolution and the power (p) during the digestion as a function of time for the Organic B-LRA process

Once the last digestion is complete, the machine system also gives a graph showing the temperature evolution during the digestion as a function of time (Figure 40).

Figure 40: Graph of the temperature evolution and the power (p) during the digestion as a function of time for the HF process

This methodology is carried out for all the samples studied in this work. It should be noted that during the digestion of the different samples such as MI38, MI67 and the filters, only one Teflon vessel was used per sample. Whereas for the natural samples, six Teflon vessels were used per sample as it was impossible to put too much sample in one vessel. Once the digestion is complete, the contents of the vessels are poured into Teflon beakers in order to move on to the next stage, evaporation.

3.3   Evaporation

The following step consists of evaporating the acids present in the solution to obtain a dry residue containing the analyte of interest. The process is fairly simple to set up but requires some care. It consists of placing the different Teflon beakers on a hot plate without exceeding 120 °C in order to avoid volatile losses of polonium (Figure 41). Teflon beakers are used because HF is able to dissolve glass beaker. It is important to note that a certain amount of tracer (Po-209) is added to the solution. This makes it possible to determine the chemical recovery and thus evaluate the losses in the next steps. This tracer must have certain characteristics. The tracer must be an isotope of the element to be measured and therefore have a physicochemical behaviour close to the element to be measured. It must also have a relatively long half-life compared to the duration of the chemical treatment in order to minimise corrections over time and optimise chemical recovery. It must also be chemically stable over time and have a high chemical purity to avoid any possible interference with the elements to be measured [35]. Alpha radiation from Po-210 emits an energy of the order of 5,304 MeV. Po-209 has a half-life of 102 years and its alpha radiation emits with an energy of the order of 4,883 MeV, while for Po-208, with a half-life of 2,898 years, its alpha radiation emits at 5,115 MeV [9]. It is therefore more advisable to use Po-209, as there is less interference at the peak energies with Po-210 [35]. For the inter-comparison samples, 0,5 ml of tracer is added before the evaporation. For the other samples, 0,1 ml of tracer in added. The specific activity of the Po-209 tracer is 0,8 Bq/ml.

The evaporation is carried out in a fume hood to avoid any inhalation of acidic fumes and to ensure a good evacuation of these fumes. Once the solution has evaporated, 2 ml of HCl is added to clean the dry residue and is evaporated again. This step is carried out 2-3 times. The duration of the evaporation will depend on the volume of the solution in the teflon beaker. The

higher the volume, the longer the evaporation will take. The duration can vary from 2 to 24 hours.
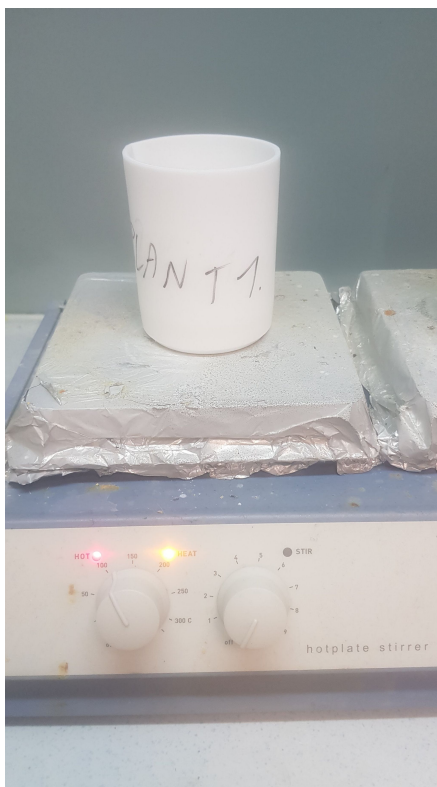
Figure 41: Evaporation set up

3.4 Filtration

Before filtration, 2 ml of HCl and about 5 ml of demineralised water are added to the beaker to solubilise the analytes (Po-209 and Po-210) present in the dry residue. Filtration consists of passing the solution through a cellulose fibre filter (Figure 42) in order to remove the last solid residues.

Figure 42: Filter Papers 42 ashless diameter 55 mm from Whatman

It is possible that insoluble actinide hydroxides may be deposited on the surface of the container, hence the need to filter the solution. This step is only possible after evaporation because the presence of HF in the solution after digestion prevents the direct use of filtration as HF is able to dissolve the glass of the filtration system. The Figure 43 shows how the filtration is carried out. The filtered solution is collected in a glass beaker.
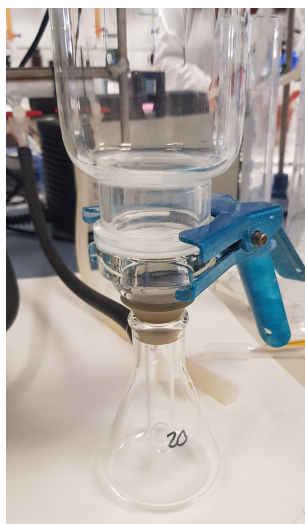
Figure 43: Filtration set up

3.5 Polonium deposition

After finishing with the digestion of the samples, evaporation and filtration the last step before measurement by alpha spectrometry is the radiochemical separation procedure of the polonium present in the solutions. The method used in this work is very similar to the method described by Flynn.

After recovering the solution from the filter, 5 ml of Hydroxylamine Hydrochloride 20% is added to reduce the iron present (Fe(III) to Fe(II)) in order to prevent it from depositing on the silver disc [17]. Without the addition of this essential element, the deposition of iron on the disc would lead to a decrease in resolution during the alpha spectrometry measurement. Next, 2 ml of Sodium citrate 20% and 10 mg of Bi carrier is added. The sodium citrate is added to act as a complexing agent for the telluride which could form a black deposit on the plate. Bismuth is added to avoid interference from Bi-212 which could be deposited with the polonium [17]. Finally, demineralised water is added to obtain a diluted solution of 50 ml. It is also important to adjust the pH to 2 with ammonium as it is important that the deposition takes place in an acidic environment to avoid hydrolysis.

Once the solution is ready, the next step is to prepare the silver plate. The silver plate will serve as a spectrometric source. Indeed, this spectrometric source must consist of a solid substance (metal) on the polished side of which the radioactive element is deposited by adhesion. The silver plate is first cleaned with a metal cleaner and then washed with soap. Then one side of the plate is covered with adhesive tape to prevent the silver from being deposited on both sides.

After the preparations, the deposition process can begin. First, the solution is heated to 85-90°C and stirred with a Teflon stirrer for 2-3 minutes. Then the silver plate is placed in the bottom of the beaker with the adhesive side down. The solution continues to be heated for approximately 90 minutes at 85-90°C. It is important to remove any air bubbles that form in order to improve deposition efficiency. The Figure 44 shows the set-up used during deposition in the laboratory.
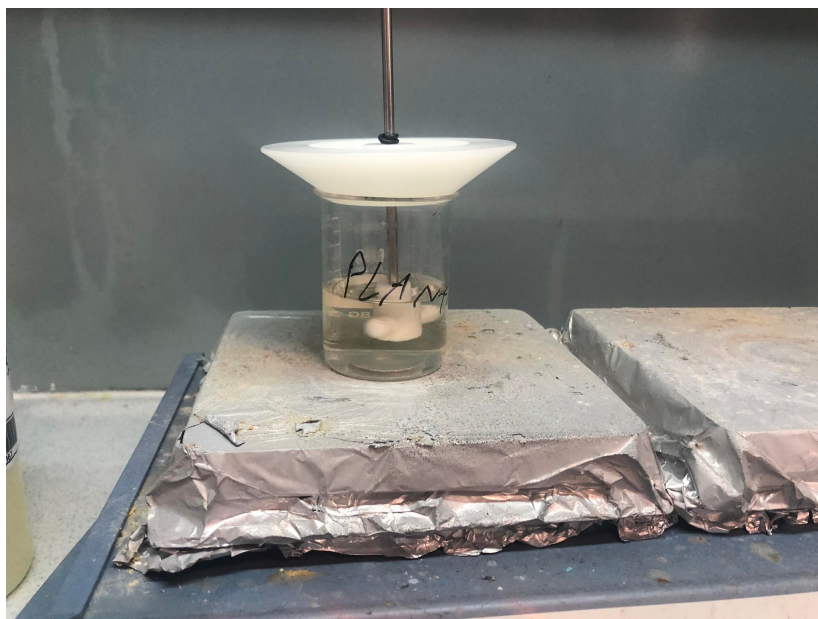
Figure 44: Deposition set up

Once deposition is complete, the plate is removed with tweezers and cleaned with deionised water and alcohol. Once dry, the plate is placed in a small petri dish and is ready for alpha spectrometry (Figure 45).
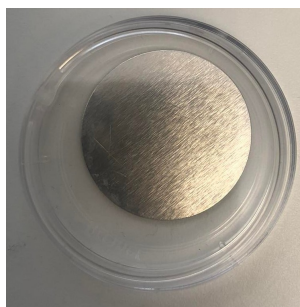
Figure 45: Silver plate in petri dish after deposition

4   Alpha spectrometry

Polonium is an alpha emitter, so it is only logical that alpha spectrometry is used to determine its activity. Moreover, liquid scintillation is a problem due to the superposition of Po-210 and Po-209 peaks. Alpha spectrometry provides the intensity of alpha radiation, i.e. the number of particles emitted in a given time (counts) as a function of their energy. The detector used in alpha spectrometry is a silicon detector.

The alpha spectrometry equipment used consists of seven vacuum chambers with their corresponding alpha detectors. The model of the spectrometer is Alpha Ensemble from Ortec. Only two of them were used in this work (ENS-U450 from ORTEC). The Figure 46 show the two detector used.

The silver plate is placed inside the chamber containing the detector. A vacuum is created in the chamber to minimise the absorption of alpha radiation energy by the air. The counting time for each measurement is 300.000 [s] in order to have a sufficient number of counts. Then the
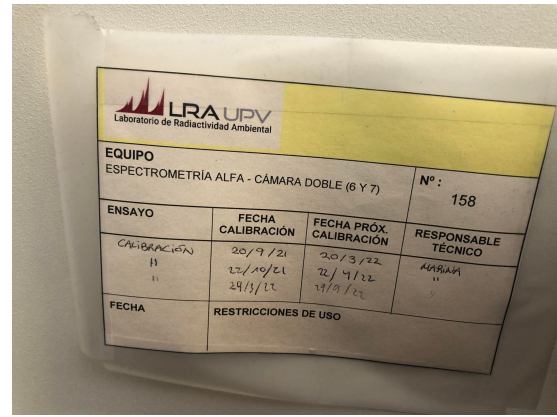
Figure 46: Alpha detector number A6 and A7 of the LRA at UPV

acquisition is started to obtain a spectrum containing the Po-209 and Po-210 peaks (if present). It is clear that before launching these measurements certain preparations are necessary. Indeed, an energy and efficiency calibration as well as a background measurement must be performed.

4.1 Calibration of the detector

First of all, it is necessary to calibrate the alpha spectrometry equipment to ensure a correct interpretation of the results. On the one hand, there is calibration in energy and on the other hand, calibration in efficiency, both of which must be carried out before the sample measurements are made. To carry out the calibration, it is necessary to have a standard of known energy and activity, certified by a laboratory of recognised prestige. The LRA-UPV has a triple source composed of U-233 , Pu-(239+240) and Am-241 (Certified by CIEMAT.[6]) A brief explanation of the calibrations mentioned is given below.

4.1.1 Energy calibration:

Energy calibration is normally performed with a radioactive source containing at least two nuclides, with distinct and known emission energies in the energy region of interest. The energy calibration method is based on assigning the known energy of the standard radionuclide to the channel of the spectrum in which it appears. A linear relationship is given between them and can be approximated by a straight line with a keV/channel slope. However, a quadratic approximation is made, which proves to be more accurate. The expression used is shown below at equation 18:

$$E[keV] = A + B.Channel + C.Channel^2 \qquad (18)$$

A system of three equations with three unknowns (A, B and C) is given for the triple source.

4.1.2 Calibration in efficiency:

Not all alpha particles emitted by the source are detected by the equipment. The detection efficiency is characterised by the ratio of the number of particles detected to the number of particles emitted. In other words, it is the ratio between the pulses generated in the detector for each incoming alpha particle (called counts per second) and the actual activity of the source

---

[6]Centro de Investigaciones Energéticas, Medioambientales y Tecnológicas

(measured in Bq). Thus, the detection efficiency or detection performance is expressed as in the equation 19:

$$RD = \text{Detector efficiency} = \frac{Cps_F - Cps_N}{A_F} \qquad (19)$$

- Cps_F = Number of alpha detection per second from the triple peak of the U-233, the Pu-(239+240) and from the Am-241

- Cps_N = Number of alpha detection per second from the background from the triple peak

- A_F [Bq]= Activity of the triple peak of the U-233, the Pu(239+240) and from the Am-241 = 242,6 Bq

The efficiency of a detector depends on the type of detector used, the geometry of the source preparation, and the distance between the source and the detector. An increase in efficiency is reflected as the sample approaches the detector. However, a distance that is too small can lead to a measurement error because the alpha particles do not strike the detector perpendicularly, resulting in a deterioration of the peak resolution. The aim is therefore to find a source-detector distance that allows good resolution without the detection efficiency being too low. The cameras used in the LRA-UPV have a fixed source-detector distance [1].

4.2 Background noise

Determining the background of the equipment, i.e. taking into account possible contributions from the instrumentation itself or from other causes, plays an important role in the processing of environmental samples with low levels of radioactivity. Very low background values are required so that they do not interfere with the measurements and the detection limits are not increased. The background is determined using the same media as the samples but without any deposition. Thus the hits detected by the detector necessarily come from the background noise.

5 Calculation of the Specific Activity

For the calculation of the specific activity A of Po-210, in Bq per sample quantity, the following equation 20 has to be used:

$$A = \frac{cps_S - cps_{BGS}}{RT \cdot M} \qquad (20)$$

$$RT = \text{Total Separation Efficiency} = \frac{cps_{tra} - cps_{BGtra}}{A_{tra} \cdot V_{tra}} \qquad (21)$$

With:

- A: Specific activity of Po-210 [Bq/kg] or [Bq/m^3]

- cps_S: Count per second of the sample's peak [count/s]

- cps_{BGS}:Count per second of the background in the sample's peak region [count/s]

- M: Quantity of sample analysed [kg] or [m³]

- RT: Total separation efficiency calculated with the equation 21

- cps_{tra}: Count per second of the tracer's peak [count/s]

- cps_{BGtra}: Count per second of the back ground in thes tracer's peak region [count/s]

- A_{tra}:Specific Activity of the Po-209 tracer = 0,8 Bq/L

- V_{tra}: Volume of tracer added: 0,5 ml for inter comparison samples and 0,1 ml for natural samples.

The total separation efficiency takes into account both the chemical efficiency of the separation and the detector efficiency. Thus, to quantify the chemical recovery (or yield) of the separation (RQ), the quotient of the total efficiency (21) and the detector efficiency (19) is calculated by the following equation 22.

$$RQ(\%) = \frac{RT}{RD} \cdot 100 \tag{22}$$

5.1 Uncertainty

The uncertainty in the specific activity $(u(A))$ is calculated from equation 23. This is the quadratic uncertainty taken by taking into account the uncertainty in the number of counts per second of the sample peak $(u(cps_S))$, the number of counts per second of the background in the region of the sample peak $(u(cps_{BGS}))$, the total efficiency $(u^2(RT))$, and the sample quantity $(u(M))$.

$$u(A) = A \cdot \sqrt{\frac{u^2(cps_S) + u^2(cps_{BGS})}{(cps_S - cps_{BGS})^2} + \frac{u^2(RT)}{RT^2} + \frac{u^2(M)}{M^2}} \tag{23}$$

The value given by this equation is the standard deviation (1σ) which indicates a confidence interval of 68%. To have a larger confidence interval, the standard deviation will be multiplied by 2 $(k = 2)$ to get 2σ which represents a confidence interval of 95.4%.

Developing the expression gives the relation to the counts per second from equation 24

$$u(cps) = \frac{u(x)}{t} = \frac{\sqrt{counts}}{t} = \sqrt{\frac{cps}{t}} \tag{24}$$

5.2 Detection limit

The detection limit is the minimum activity that can be quantified in the device. The detection limit is determined by taking into account the sample quantity, the chemical separation efficiency and the measurement time. It is possible to calculate the detection limit using the Currie method given by equation 25.

$$LD = \frac{2,71 + 4,65 \cdot \sqrt{C_{BG}}}{t_{count} \cdot RT \cdot M} \tag{25}$$

But it was decided to calculate the detection limit (LD) from the more recent and comprehensive ISO 11929 standard. The equation 26 is used to calculate this LD.

$$LD = \frac{2 \cdot a^* + \frac{(k^2 \cdot \omega)}{t_M}}{1 - k^2 \cdot u_{rel}^2(\omega)} \tag{26}$$

With:

- a^*: Decision threshold for the total activity quantity in Bq/kg or Bq/m^3, where:

$$a^* = k_{1-\alpha} \cdot \omega \sqrt{\frac{cps_{BGS}}{t_M} + \frac{cps_{BGS}}{t_F}} \tag{27}$$

Where $k_{1-\alpha}$ is a equivalent constant = 1,65

- ω: coefficient equal to

$$\omega = \frac{1}{V \cdot RT \cdot e^{-\frac{ln2}{T} \Delta t}} \tag{28}$$

Where: - V is the amount of sample analysed [L, m^3, kg] and $e^{-\frac{ln2}{T} \Delta t}$ is the time correction factor where Δt is the time elapsed from the date of deposition to the date of measurement and T is the half-life of Po-210 .

- t_M: Sample counting time [s].

- t_F: Background counting time [s].

- $u_{rel}^2(\omega)$ Relative uncertainty calculated as the sum of:

$$u_{rel}^2(\omega) = \frac{u^2(RT)}{RT^2} + \frac{u^2(V)}{V^2} \tag{29}$$

Chapter 3: Results

1 Introduction

This chapter will be devoted to the presentation of the results obtained and their analysis.

The analysis will first be devoted to the drying of the samples in order to see the percentage of mass loss during this process. Then, it will focus on the digestion of the different samples. Finally, the results and analysis of the measurements will be carried out in two stages.

Firstly, the analysis will focus on the inter-comparison samples. The aim will be to compare the experimentally obtained values with the values given in the IAEA reference documents.

Secondly, the analysis will focus on the natural samples. The aim will be to compare the values obtained experimentally with those obtained in other studies or given by competent authorities. The analysis will also check whether the Po-210 activity of these samples does not exceed the European standards for the regulation of Po-210 in nature.

2 Drying

The aim of drying is to remove almost all the water present in the samples analysed. The Table 6[7] shows all the drying operations carried out according to the type of sample. The percentage of mass loss per sample is also indicated.

Table 6: Loss of mass after drying of the samples

Name	Mass before drying [g]	Mass after drying [g]	Loss of mass [%]
MI38	2,3184	2,1876	5,6
MI67	5,7637	5,7318	0,6
Tobacco	6,677	6,1892	7,3
Fresh Grass	158,2	28,4	82,0
Gilet	14,9	14,5	2,7

The samples MI38 and MI67 were already dried and sieved by the IAEA because their mass loss is quite low, especially for MI67. This is also the case for the tobacco sample with a mass loss of 7,3%. For the soil sample from Gilet, drying had already been carried out beforehand. The only purpose of drying these 4 samples in the LRA laboratory was to remove any traces of water caused by humidity. Only the grass sample had a very high loss of mass. This is completely normal as it is a sample taken directly from nature. Therefore, it is quite normal that the water content in this grass sample is high. As a reminder, drying does not apply to filters.

3 Digestion

During digestion, only sample MI38 was difficult to handle. Indeed, the MI38 has a high organic content, for this reason the main problem during digestion was the addition of H_2O_2. Indeed,

---

[7]In the various tables of results, it was decided to keep one digit after the decimal point except for the mass measurements. Indeed, the scale used could go up to 4 digits after the decimal point. Therefore, the masses will have a precision of 4 digits after the decimal point.

the effervescence caused by this addition was very strong as shown in the Figure 47. Therefore this step was done slowly and carefully.

Figure 47: Effervescence of MI38 sample

For the other samples, the effervescence was also present but of less intensity.

The graph in the Figure 48 shows the typical sequence of the first digestion step, i.e. the Organic B_LRA programme for one sample. This graph is the same for all digested samples. The thick red line shows the actual evolution of the sample during digestion. It is supposed to follow as closely as possible the course of the thin line that represents the ideal temperature evolution. The difference between the two is normal at the beginning because the sample does not have a temperature of 0°C at the beginning of the digestion. The most important thing is that the thick red line reaches the temperature value of each step. During cooling there is also a difference between the two. The ideal temperature development during cooling is to go from the maximum to the minimum temperature directly, but this is physically impossible. This is why the actual cooling curve follows a decreasing exponential. The black curve represents the power used during digestion to heat the vessels.

► Unique ID	315
► Date and Time	4/4/2022 1:05:58 PM
► User	Administrator
► Run Note	-
► Method Name	Organic B-LRA
► Method Information	0.1 g
► Recipe	8ml HNO3 + 2ml HCl+ 2ml H2O2

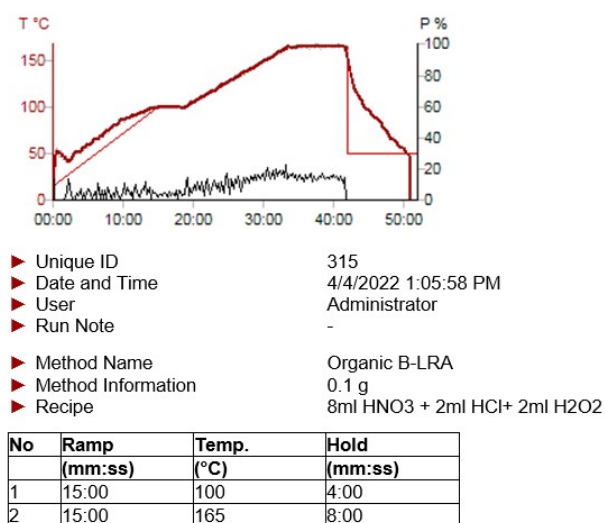| No	Ramp	Temp.	Hold
	(mm:ss)	(°C)	(mm:ss)
1	15:00	100	4:00
2	15:00	165	8:00

Figure 48: Graph of the temperature evolution and the power (p) during the digestion as a function of time for the Organic B-LRA process for MI 67 sample

The graph in the Figure 49 shows the second and final digestion step for a sample, i.e. the HF program. This graph is the same for all the digested samples and represents the same characteristics as the previous graph. The difference is only in the temperature step to be reached and the duration of the digestion.

No	Ramp	Temp.	Hold
	(mm:ss)	(°C)	(mm:ss)
1	10:00	150	5:00
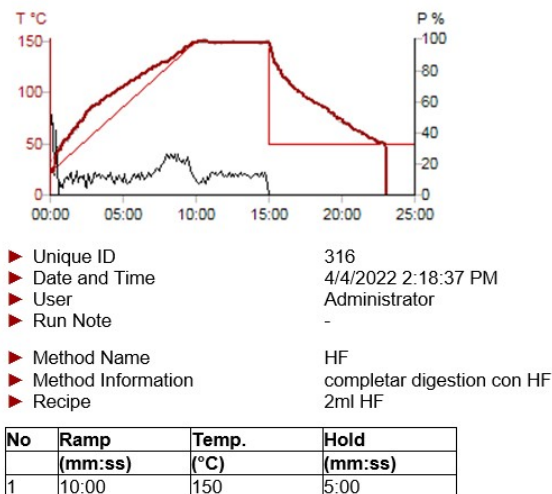
Figure 49: Graph of the temperature evolution and the power (p) during the digestion as a function of time for the HF process for MI 67 sample

4 Results and Analysis

4.1 Intercomparison sample

This section is dedicated to the analysis of the IAEA soil samples MI38 and MI67.

4.1.1 Soil MI38 samples

The Figure 50 shows the typical spectrum obtained for one of the aliquots of the MI38 sample. All other spectra have the same appearance.
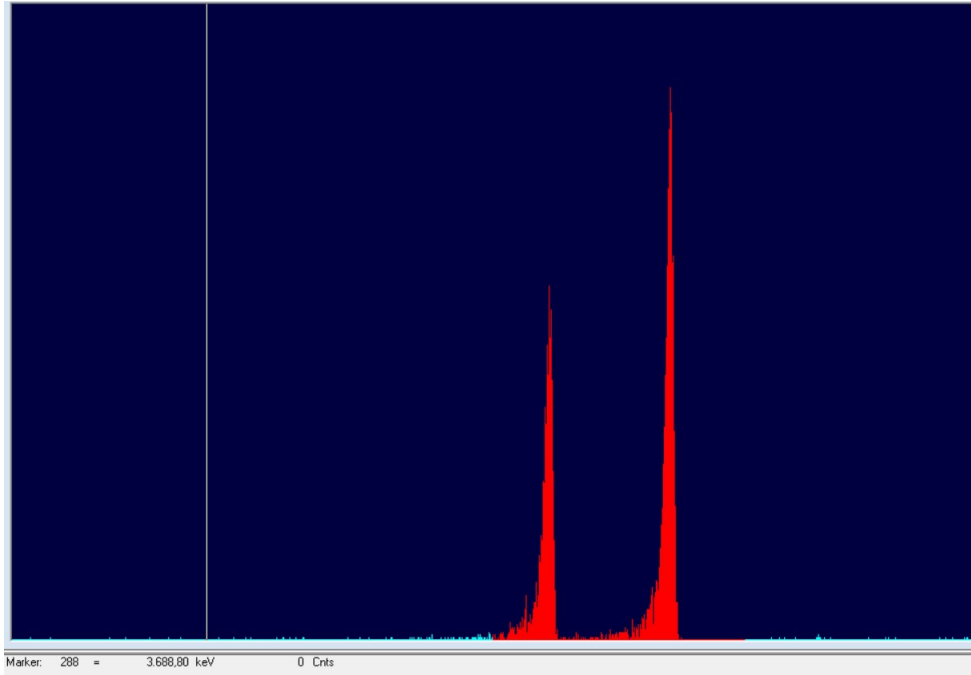
Figure 50: Spectrum of a MI38 aliquots with the Po-209 peak on the left and the Po-210 peak on the right.

The Table 7 shows the overall results obtained for the analysis of the IAEA MI38 sample. The measurements were made on 6 aliquots.

Table 7: Specific activity and chemical recovery for sample MI38

Aliquot n°	Mass [g]	A[Bq/kg]	u(A) [Bq/kg] $k = 2$	LD [Bq/kg]	RQ[%]	u(RQ) $k = 2$ [%]
1	0,2006	236,1	16,3	2,7	61,3	3,1
2	0,2013	425,1	42,0	3,6	33,6	2,5
3	0,2001	360,0	31,3	3,1	49,9	3,3
4	0,1995	456,3	28,0	2,5	77,9	4,0
5	0,2043	665,2	43,2	2,5	55,1	3,1
6	0,2012	550,8	33,7	1,5	61,6	3,2

The results show that the chemical recoveries (RQ) are higher than 49% except for one measurement with an average value of 56,6% and a relative standard deviation of 26%. The chemical recovery is variable, but the values are enough to calculate the activity of the sample with these limits of detection. The limit of detection is defined as the smallest measured activity value that can be said to be non-zero.

In terms of specific activity determination, the values obtained experimentally are close to the reference value of 430,8 Bq/kg. On the other hand, some experimental values are far from this reference value. This can be explained by the inhomogeneity of the sample. Indeed, the measurements are carried out on small quantities of polonium, so it is possible that there is a little more or less polonium from one aliquot to another. A small difference can lead to a large variation in activity.The IAEA advises to analyse at least 1g of sample to ensure homogeneity. However, the samples analysed here are about 0,2g, hence the disparity in the values obtained. On the other hand, by calculating the average of all these samples, it is possible to see that the average specific activity tends towards the reference value. By taking the average, we

exceed the minimum threshold given by the IAEA of 1g. This can be seen in the graph in the Figure 51. The mean obtained is 448,9 Bq/kg and the relative standard deviation is 33%. The deviation is a little bit high and could be explain because the amount of sample analysed is not enough to assure the homogeneity of the sample. Otherwise the relative bias (RB), calculated by the equation 30 , that compare the mean value with the inter-comparison value is about 4,2% witch is very accurate. We can say that this method worked with a good accuracy for the MI38 samples with the mean value. The problem with the repeatability is maybe due to the in-homogeneity of the sample.
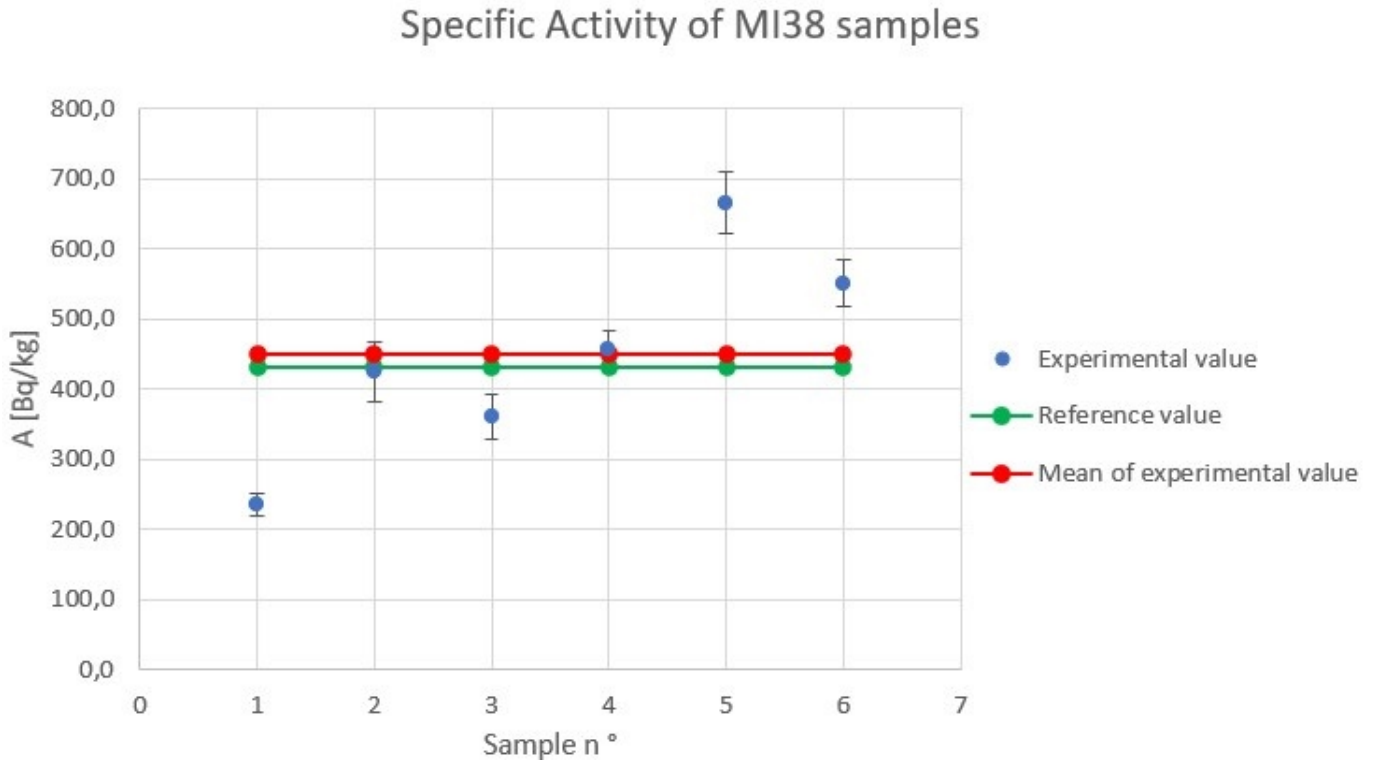

Figure 51: Specific Activity of MI38 samples

$$RB[\%] = \frac{|A_{mean} - A_{Inter-comparison}|}{A_{Inter-comparison}} \cdot 100 \qquad (30)$$

4.1.2 Soil MI67 samples

The Figure 52 shows the typical spectrum obtained for one of the aliquots of the MI67 sample. All other spectra have the same appearance.
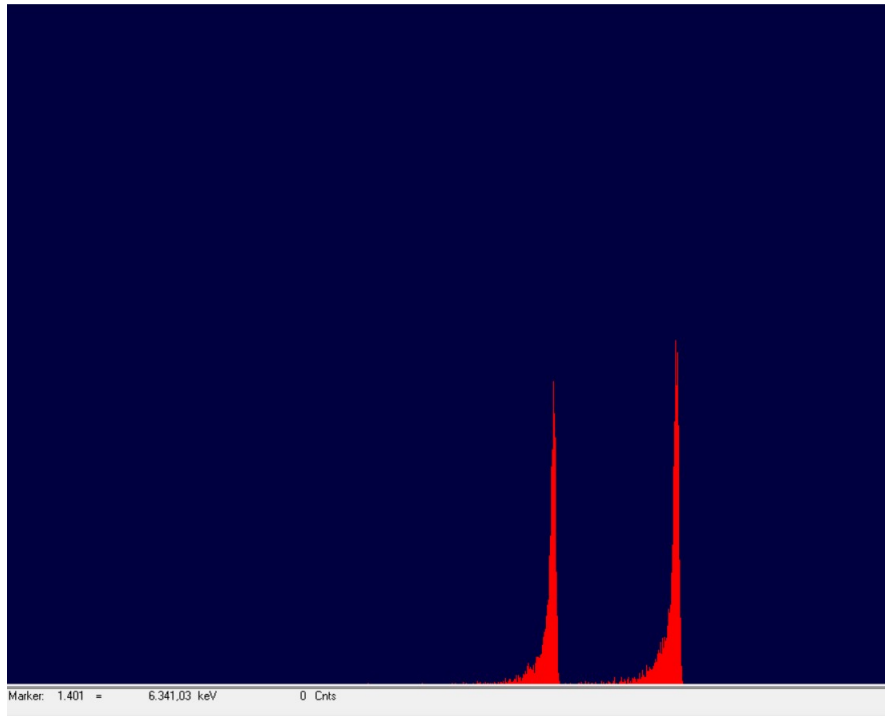
Figure 52: Spectrum of a MI67 aliquots with the Po-209 peak on the left and the Po-210 peak on the right.

The Table 8 shows the overall results obtained for the analysis of the IAEA MI67 sample. The measurements were made on 5 aliquots.

Table 8: Specific activity and chemical recovery for sample MI67

Aliquot n°	Mass [g]	A[Bq/kg]	u(A) [Bq/kg] $k = 2$	LD [Bq/kg]	RQ[%]	u(RQ) $k = 2$ [%]
1	0,2070	458,4	28,1	1,8	71,6	1,9
2	0,2006	645,2	48,5	2,2	53,0	1,7
3	0,2009	588,1	43,6	2,8	57,8	1,8
4	0,2012	508,3	39,2	0,7	62,3	2,0
5	0,2042	519,7	42,3	2,7	54,4	1,8

The chemical yields obtained are higher than 50% with an average value of 59,8% and a relative standard deviation of 12,6%, which is quite encouraging considering the volatile nature of Po-209 and Po-210. The limit of detection are very low for this contaminate sample. This limit of detection permit the quantify the activity of those samples because they are below of the measured activity.

As regards the determination of specific activities, the values obtained experimentally are all higher than the reference value of 423 Bq/kg. The mean obtained is 543,9 Bq/kg and the relative standard deviation is 13,4% as shown in the graph in Figure 53. The relative standard show that the repeatability of the measurement on this sample are quite accurate because the relative standard deviation on the mean activity is below 25%. The relative bias calculated by the equation 30 that compare the mean value with the inter-comparison value is about 29%. This value is higher than the acceptable relative bias of 25%.

The explanation for this higher relative bias can be found it the calculation on the inter-comparison value. It should be remembered that the calculation of the reference activity was

carried out using Pb-210 and not Po-210 as was the case for the MI38 sample. It was assumed that Pb-210 and Po-210 were in equilibrium, but this may not be the case. It is quite possible that there is no equilibrium. Another factor to take into account is the way the measurement was carried out on the MI67 sample. Indeed, this sample was analysed by gamma spectrometry. However, the energy emitted during the gamma decay of Pb-210 is very low, which leads to a greater uncertainty in the reference value given. These two elements combined may be the cause of this discrepancy. The results obtained showed that the secular equilibrium between Pb-210 and Po-210 was not established in the MI67 sample.
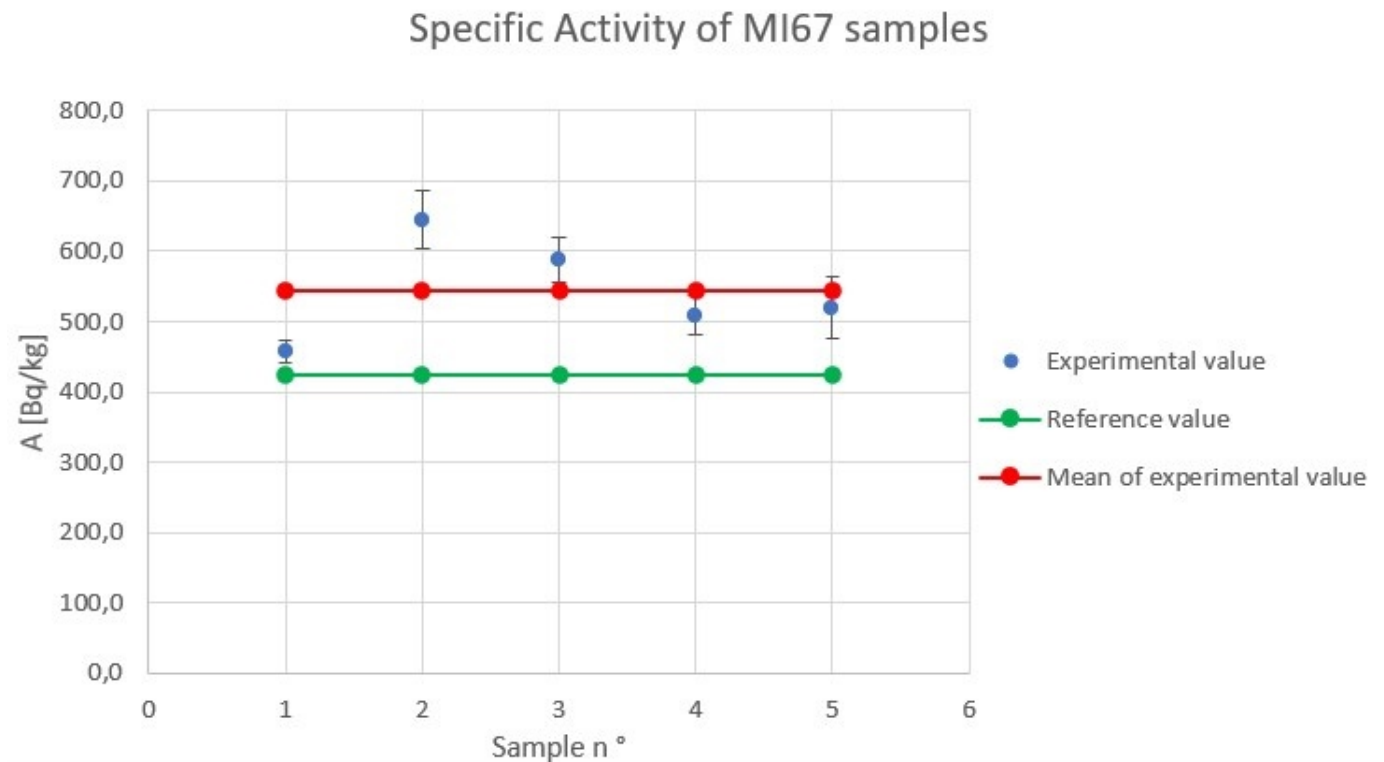

Figure 53: Specific Activity of MI67 samples

4.2 Natural Samples

This part will be devoted to the analysis of natural samples. The objective will be to calculate the specific activity of Po-210 in these samples to see if they are below the exemption values given by the European directives and to test the method for type of environmental matrices. These measurements will be used to check whether objectives 3 and 15 of the Sustainable Development Programme are met.

4.2.1 Aerosols: Filters

The Figure 54 shows a typical spectrum obtained for one filter.

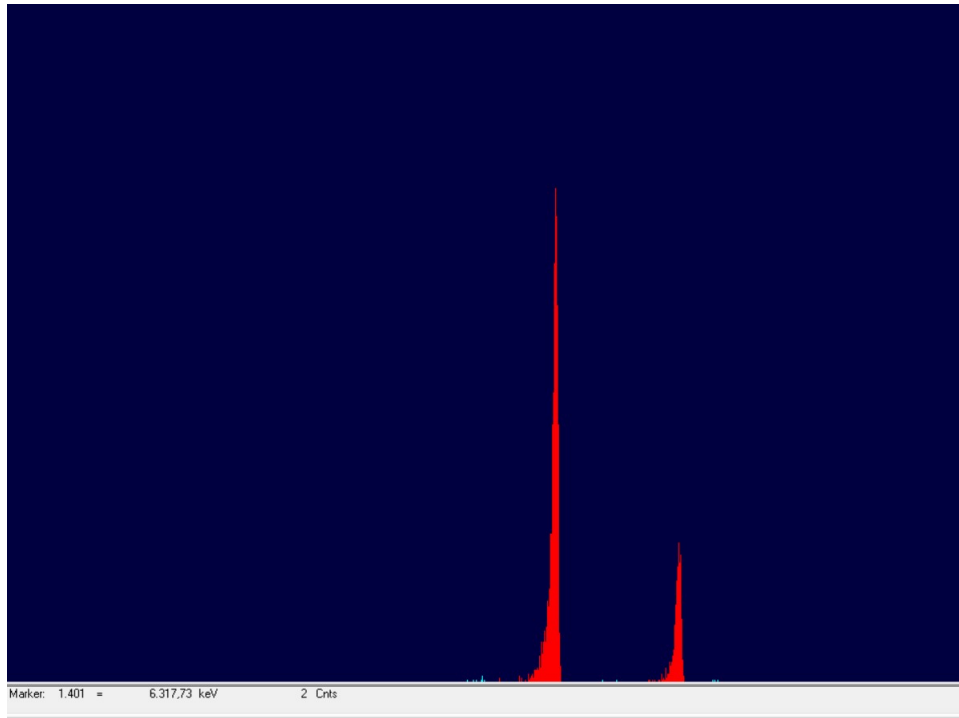Marker: 1.401 =   6.317,73 keV   2 Cnts

Figure 54: Spectrum of a Filter sample with the Po-209 peak on the left and the Po-210 peak on the right.

The results of the measurements on the two different types of filters are shown in the Table 9 and 10. The average chemical yield is 48% and the relative standard deviation is about 31%. This low recovery is explained by the fact that the tracer is placed just before evaporation, thus causing more loss, unlike most of the scientific literature where the tracer is placed just before deposition. The choice of placing the tracer during evaporation was motivated by a desire to be as accurate as possible. On the other hand, adding the tracer before digestion had certain defects. Indeed, the tracer (Po-209) being in liquid form and the Po-210 present in the samples in solid form, they would not have behaved in the same way during digestion. It is essential that the tracer has the same physico-chemical behaviour as the element measured.

The limit of detection are very low for this natural sample. This limit of detection permit quantify the activity of those samples because they are below of the measured activity.

Table 9: Specific activity for Filters sample

Ali. n°	Vol. of air $[m^3]$	A[Bq/m^3 x 10^{-4}]	u(A) [Bq/m^3 x 10^{-4}] $k = 2$	LD [Bq/m^3 x 10^{-5}]
1	414,03	2,63	0,52	0,13
2	499,00	2,43	0,47	0,09
3	412,92	4,39	0,88	0,03
4	342,01	0,69	0,06	0,12
5	431,39	0,51	0,10	0,09
6	336,49	3,44	0,70	0,01
7	434,31	2,64	0,54	0,16

Table 10: Chemical recovery for Filters sample

Ali. n°	RQ[%]	u(RQ) $k = 2$ [%]
1	49,33	9,57
2	59,80	11,38
3	40,89	8,11
4	51,54	2,78
5	72,69	13,58
6	37,89	7,58
7	36,96	7,43

In terms of the specific activity of the aerosols present on the filters, the graph of the Figure 55 shows the specific activity per filter type. The specific activity values are between 2 and 5[Bq/m³ x 10^{-4}] for the majority of the values. Only two values are quite low. In order to find out whether these values are due to very low aerosol activity or to the filter's own activity, two additional measurements were carried out on a blank filter of each type. The results obtained on the blank filters show that the specific activity of the filters is of the order of µBq/m³. The specific activity of the two low values is indeed caused by the aerosols captured on the filters. The low limit of detection obtained can also confirm that supposition.

Figure 55: Specific activity in filters samples containing aerosols

When we see that the mean of the specific activity is about 2,3 [Bq/m³ x 10^{-4}] and that the relative standard deviation is about 73%, the question that we have to ask is why there is such a difference between the values ? The graph on the Figure 56 shows the result for the filters as a function of the date and the type of pump used. The values obtained by the

filters placed in pump n°1 are slightly higher compared to those of pump n°2. This result is not surprising as pump n°1 is closer to the window which increases the probability of sucking in more aerosols compared to pump n°2 which is a little lower. However, the difference in values obtained between the two pumps is not very significant. Indeed, the order of magnitude obtained is the same.

We also notice that the values obtained are different depending on the date. The specific activity between two filters measured on the same date is almost identical. The only difference is the use of a different pump as explained above. The difference in specific activity between the different dates is due to climatic variations.
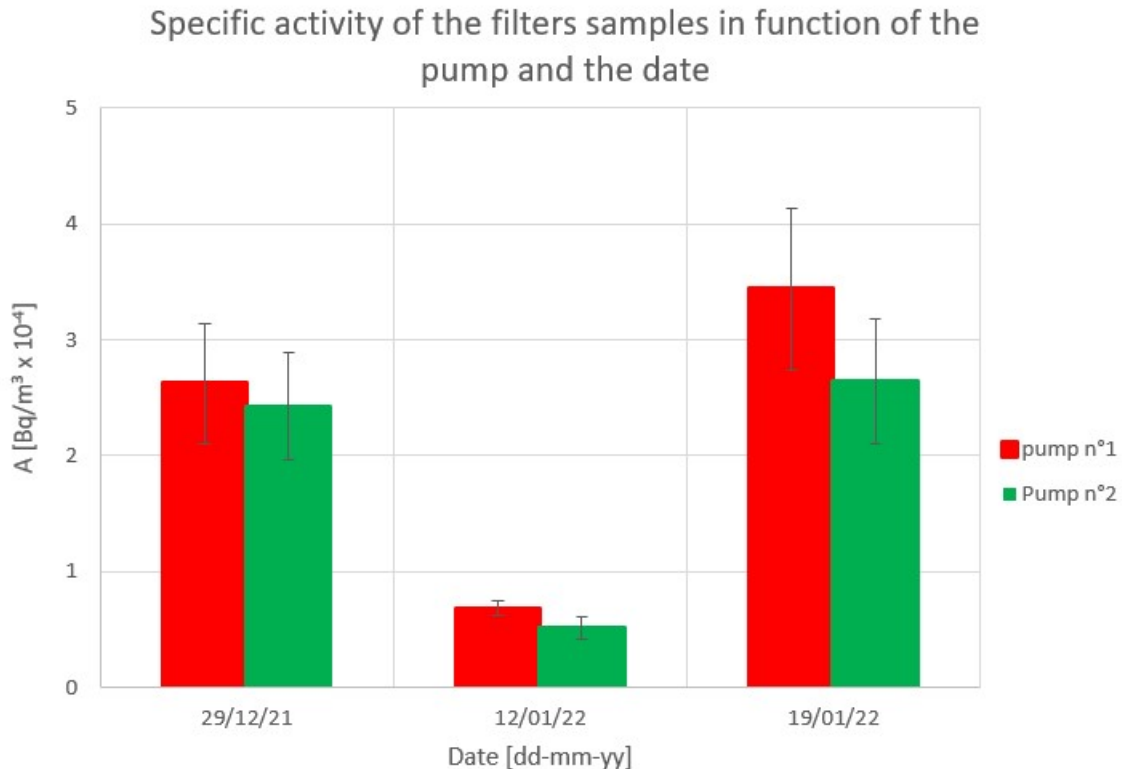

Figure 56: Specific activity of the filters samples in function of the pump and the date

The overall results are in the order of 10^{-4} Bq/m^3, which is the reference value of 0,05 mBq/m^3 given by UNSCEAR [19]. These results show that the air is not highly contaminated by Po-210. Good air quality (regarding Po-210 levels) is important in order to comply with the Sustainable Development Programme objectives 3 and 15. To finish, we do not know the activities at the sampling date because the filters were analysed several months after (5 month later). We could not calculate the activity at the sampling date because maybe there is also Pb-210 making increase the activity of Po-210. It is very difficult to calculate the activity at the sampling date moment due to the desintegration chain.

4.2.2 Tobacco

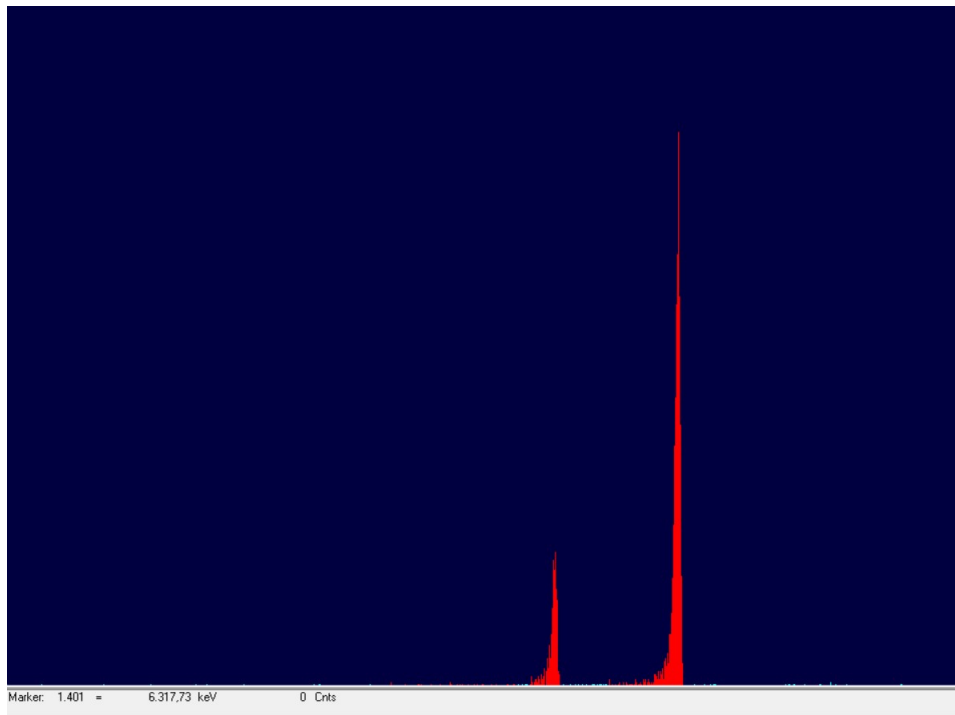The Figure 57 shows a spectrum obtained from a tobacco sample.

Figure 57: Spectrum of a tobacco sample with the Po-209 peak on the left and the Po-210 peak on the right.

Two tobacco samples were processed. The Table 11 shows the results obtained. The first remarkable thing is the difference in chemical yield between the two values. This variation in chemical yield is rather complicated to explain. Indeed, the behaviour of Po is quite complex. Sometimes good chemical yields are obtained and sometimes not. One way to do this would be to carry out an in-depth research on the behaviour of Po. Polonium is a very difficult element to pin down. Especially since putting the tracer on before evaporation can lead to losses. It must be taken into account that the quantities analysed are very small, the loss of even a single drop of solution can have a huge impact on the chemical yield.

The limit of detection are very low for this natural sample. This limit of detection permit the quantify the activity of those samples because they are below of the measured activity.

Table 11: Specific activity and chemical recovery for tobacco sample

Aliquot n°	Mass [g]	A[Bq/kg]	u(A) [Bq/kg] $k = 2$	LD [Bq/kg]	RQ[%]	u(RQ) $k = 2$ [%]
1	2,9874	16,9	3,2	0,1	83,1	15,4
2	3,1040	20,4	4,0	0,1	48,5	9,4

As far as the values obtained are concerned, it can be seen that the values are quite similar as shown in the graph in the Figure 58. The average value of the activity is 18,7 Bq/kg and the relative standard deviation is about 13,3% which is very accurate. Indeed, these values are within the range observed by different countries. In Egypt the Po-210 activity in tobacco varies between 14,8 and 27,2 Bq/kg, in Greece it varies between 3,6 and 17 Bq/kg [42]. While in Brazil it varies between 11,9 and 30,2 Bq/kg [43]. The study of Po-210 in tobacco and tobacco itself is extremely important in the fight for wellbeing and health (objective n°3) as tobacco is one of the main causes of lung cancer in the world. The accuracy of this method used on this tobacco sample are quite into the range of other measurement assessed by other scientifically.
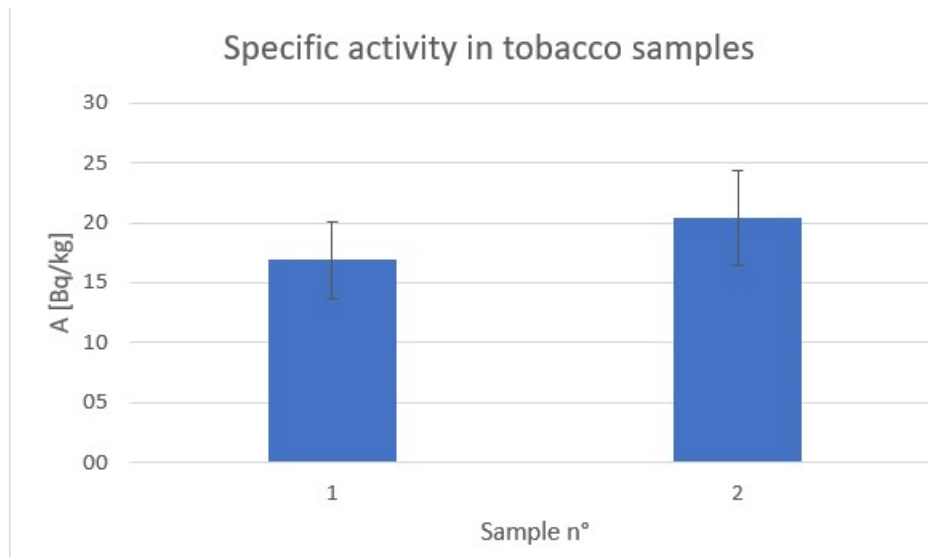
Figure 58: Specific activity in tobacco samples

4.2.3 Grass from UPV

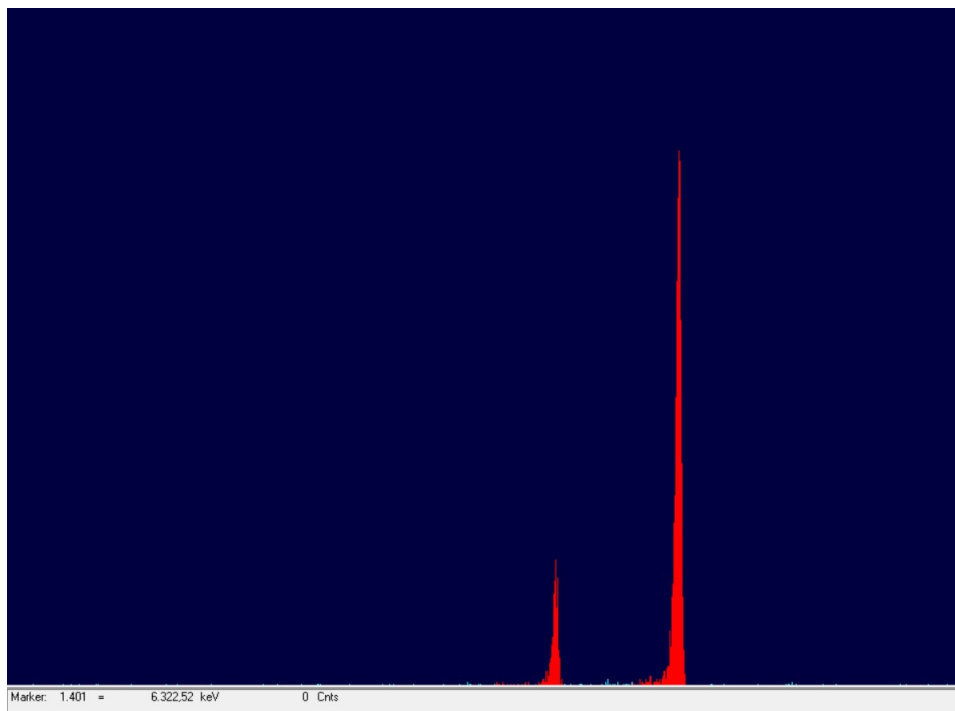The Figure 59 shows the typical spectrum obtained for a grass sample from the UPV.

Figure 59: Spectrum of a grass sample from UPV with the Po-209 peak on the left and the Po-210 peak on the right.

The Table 12 shows all the results obtained for the 3 aliquots of the analysed grass sample. The chemical yields are quite disparate. The average chemical yield is 58% and the relative standard deviation is about 32%. This again shows the unpredictable behaviour of Po-210.

The limit of detection are very low for this natural sample. This limit of detection permit the quantify the activity of those samples because they are below of the measured activity.

Table 12: Specific activity and chemical recovery for grass sample

Aliquot n°	Mass [g]	A[Bq/kg]	u(A) [Bq/kg] $k = 2$	LD [Bq/kg]	RQ[%]	u(RQ) $k = 2$ [%]
1	2,3646	19,6	3,7	0,2	79,2	14,7
2	2,2729	25,8	5,2	0,2	43,4	8,4
3	2,3384	30,2	6,1	0,1	52,7	10,3

The calculated specific activity values are quite close to each other taking into account the uncertainties as shown in the graph in the Figure 60. The average value on the activity is 25,2 Bq/kg and the standard deviation is about 21% wich is accurate (lower than 25%). These values are also close to the values obtained for tobacco. Nevertheless, these values are very low and do not have a great effect on human health as the grass is not consumed.
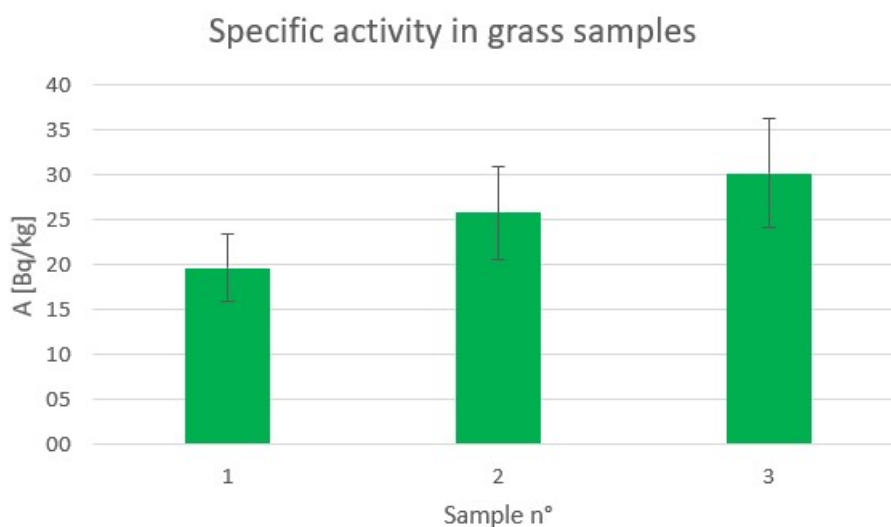

Figure 60: Specific activity in grass samples

4.2.4 Soil from Gilet

The Figure 58 shows the typical spectrum obtained for a soil sample from Gilet.
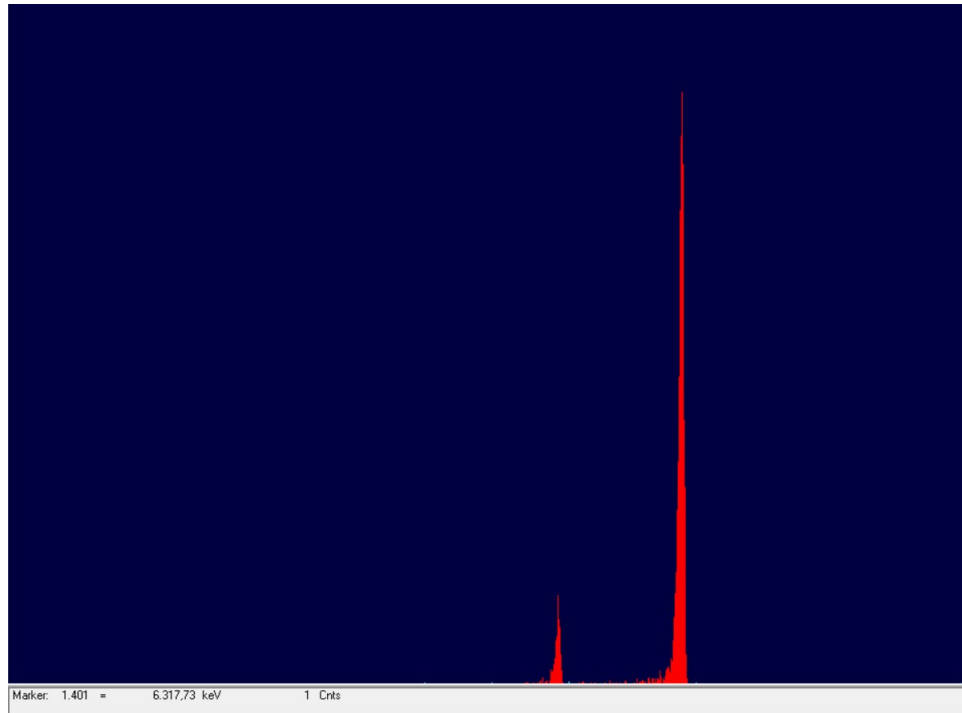
Figure 61: Spectrum of a soil sample from Gilet with the Po-209 peak on the left and the Po-210 peak on the right.

The Table 13 shows all the results obtained for the 3 aliquots of the Gilet soil sample analysed. The average chemical yield is 37% and the relative standard deviation is about 36%, probably for the reasons discussed above.

The limit of detection are very low for this natural sample. This limit of detection permit the quantify the activity of those samples because they are below of the measured activity.

Table 13: Specific activity and chemical recovery for Gilet soil sample

Aliquot n°	Mass [g]	A[Bq/kg]	u(A) [Bq/kg] $k = 2$	LD [Bq/kg]	RQ[%]	u(RQ) $k = 2$ [%]
1	1,2921	167,2	35,4	1,3	28,6	6,0
2	1,2266	124,9	25,6	1,1	29,7	6,0
3	1,2253	102,1	19,9	0,5	52,1	10,0

For the specific activity in Po-210 of these three aliquots, the graph in the Figure 62 shows that the values obtained are slightly different. But taking into account the uncertainty, it can be seen that these values are not so far apart. The average of the activity is 131,4 Bq/kg and the relative standard deviation is about 25,1%. This slight difference can be explained by the inhomogeneity of the soil sample analysed. As mentioned before, the activity values are very low and therefore so is the amount of Po-210 in the samples. This means that a slight variation in Po-210 concentration between soil aliquots can lead to a variation in the specific activity. However, the values are quite high for this type of soil.

Gamma-ray spectrometry measurements carried out by the LRA show that the average Pb-214 activity is 21,1 Bq/kg. Since Pb-214 also comes from the decay chain of uranium and is supposed to be in secular equilibrium with it, the U-238 activity of the soil is also about 21,1 Bq/kg. The question that needs to be asked is how come the Po-210 activity is so high? Indeed, Po-210 should be in secular equilibrium with U-238, but this is not the case. Moreover, if there

was a radon leak that could break the secular equilibrium, the Po-210 activity should be lower. The most likely reason for the high Po-210 activity in this soil sample is atmospheric fallout. Indeed, it is quite possible that some Po-210 is present on the soil surface due to atmospheric fallout containing Po-210-contaminated aerosols. The LRA also measured Pb-210 activity of the order of 10^2 Bq/kg in a soil sample from Gilet. Pb-210 seem to be in equilibrium with Po-210. This value is of the same order of magnitude as the values obtained for the Gilet soil aliquots.
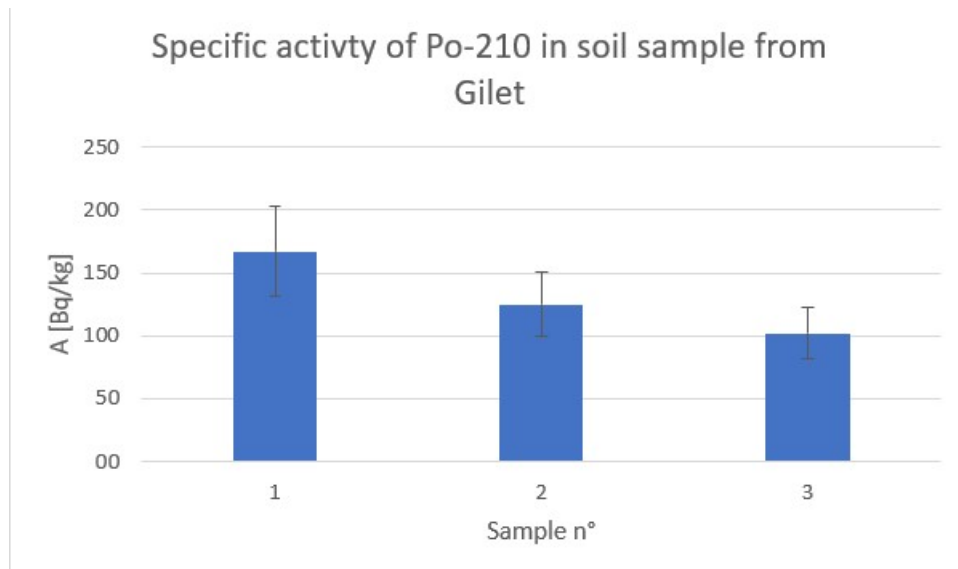

Figure 62: Specific activty of Po-210 in soil sample from Gilet

Chapter 4: Conclusion

This work has highlighted the importance of measuring Po-210. As it is highly radiotoxic to living organisms, its study is essential and fits perfectly with objectives n°3 and n°15 of the Sustainable Development Programme.

It has shown the complexity of developing an efficient and rapid method in case of emergency. Indeed, the method developed still contains some points for improvement.

First of all, the time needed to carry out the analysis depends very much on the type of sample analysed. The Figure 63 shows the different steps in the process and an estimate of their duration. For contaminated samples, such as intercomparison samples, the time is shorter. On the other hand, in the measurement of natural samples with low activity, the execution time is longer. The most time consuming steps for natural samples are evaporation and alpha spectrometry. In order to obtain a good measurement, a sufficiently high amount of natural sample must be taken to be above the detection limit. However, by increasing the sample mass, the time required for evaporation after digestion is higher than for intercomparison samples. In spectrometry, the counting time for natural samples is higher than for intercomparison samples because the activity is very low. The time needed to perform the method therefore depends greatly on the contamination of the sample. The more contaminated the sample, the faster the method will be performed.

Figure 63: Process steps and an estimate of their duration

Secondly, the chemical yields are not always high and constant. The causes of these variations are probably caused by a combination of different factors such as the not really well known behaviour of polonium in solution, the volatility of Po-210 and Po-209 and incidental losses during the different steps. It is as important to note that the chemical yields are lower than those obtained in the scientific literature because the majority place the tracer before deposition and not from evaporation. It is therefore normal that the chemical yield is lower.

On the other hand, the results obtained for the activities are quite encouraging. The results obtained are quite consistent with the values found in other works. The slightly different values are not outliers either.

This means that this method can be very interesting for the calculation of Po-210 in natural samples. It is obvious that further research and measurements are needed to optimise the method. Further work would therefore be very interesting in order to further develop this method and to improve the basis provided in this work.

Chapter 5: Bibliography

Bibliography

[1] LORENA LAFUENTE HERNÁNDEZ. *OPTIMIZACIÓN DE UN PROCEDIMIENTO DE DIGESTIÓN EN MUESTRAS AMBIENTALES CON HORNO MICROONDAS Y SU APLICACIÓN A LA SEPARACIÓN RADIOQUÍMICA DEL PO-210.* 2017.

[2] ONU. *Department of Economic and Social Affairs Sustainable Development.* May 2022. URL: https://sdgs.un.org/.

[3] Glenn F. Knoll. *Radiation Detection and Measurement: Fourth edition.* WILEY, 2010.

[4] toppr. *plot number of neutrons vs protons for radioactive decay.* https://www.toppr.com/ask/content/story/amp/plot-number-of-neutrons-vs-protons-for-radioactive-decay-101213/.

[5] C.Ngo C.Le Sech. *Physique nucléaire, des quarks aux applications.* 2st ed. Dunod, 2020.

[6] W. Wacławek M. Wacławek. "Marie Skłodowska-Curie her contributions to chemistry radiochemistry radiotherapy". In: *Analytical Bioanalytical Chemistry 400* (2011), pp. 1567–1575. DOI: 10.1007/s00216-011-4922-6.

[7] Ansoborlo E. Berard P. Auwer Den C. Leggett R. Menetrier F. Younes A. Montavon G. Moisy P. "Review of Chemical Radiotoxicological Properties of Polonium for Internal Contamination Purposes." In: *Chemical Research in Toxicology 25* (2012), pp. 1551–1564. DOI: 10.1021/tx300072w.

[8] Change Tan. "Big Gaps and Short Bridges: A Model for Solving the Discontinuity Problem". In: *Answers Research Journal* (2016).

[9] N.K. Sethy A.K. Sutar P. Rath V.N. Jha P.M. Ravi R.M. Tripathi. "A review of radio chemical analysis and estimation of 210Po in soil matrices". In: *Elsevier* (2015), pp. 590–596. DOI: 10.1016/j.jrras.2015.07.001.

[10] Vogelsang W.F. White A.M. Wittenberg L. Sze D.K. *Polonium Production in the MARS Reactor.* University of Wisconsin. 1984.

[11] Hermanne A Tárkányi F Takács S Szücs Z Shubin Y.N. Dityuk A.I. "Experimental study of the cross-sections of alpha-particle induced reactions on 209Bi". In: *Applied Radiation Isotopes 63* (2005), pp. 1–9. DOI: 10.1016/j.apradiso.2005.01.015.

[12] : F. Coppin S. Roussel-Debet. "FICHE RADIONUCLÉIDE: Polonium 210 et environnement". In: *IRSN* (2004).

[13] B.R.R. Persson. "210Po and 210Pb in the Terrestrial Environment". In: *Current Advances in Environmental Science* (2014), pp. 22–37.

[14] Carvalho F. Fernandes S. Fesenko S. Holm E. Howard B. Martin P. Phaneuf M. Porcelli D. Prohl G. Twining J. *The Environmental Behaviour of Polonium.* IAEA. 2017.

[15] Baize D. Tercé M. "Les éléments traces métalliques dans les sols: Approches fonctionnelles et spatiales". In: *Quae* (2002).

[16] Horváth M. Ipbüker C. Hegedűs M. Kovács T. Tkaczyk A.H. "Development of measurement system for adsorption of long-lived radon decay products on the leaf surface of tobacco plants." In: *Journal of Radioanalytical and Nuclear Chemistry 313* (2017), pp. 391–400. DOI: 10.1007/s10967-017-5327-6.

[17] Thi Hong Hanh Le. "Distribution et comportement du polonium dans deux anciens sites miniers français". PhD thesis. Institut de Chimie de Nice, 2020.

[18] F. COPPIN s. ROUSSEL-DEBET. "Comportement du 210Po en milieu terrestre : revue bibliographique". In: *Radioprotection 2004 Vol. 39, no 1* (2004), pp. 221–227.

[19] United Nations Scientific Committee on the Effects of Atomic Radiation UNSCEAR 2000 Report to the General Assembly. *SOURCES AND EFFECTS OF IONIZING RADIATION*. VOLUME I: SOURCES. UNITED NATIONS, 2000.

[20] Al-Masri M.S. Amin Y. Ibrahim S. Al-Bich F. "Distribution of some trace metals in Syrian phosphogypsum". In: *Applied Geochemistry 19* (2004), pp. 747–753. DOI: 10.1016/j.apgeochem.2003.09.014.

[21] Fernando Santos-Frances Elena Gil Pacheco Antonio Martínez-Grana Pilar Alonso Rojo Carmelo Avila Zarza Antonio García Sanchez. "Concentration of uranium in the soils of the west of Spain". In: *Environmental Pollution Volume 236* (2018), pp. 1–11. DOI: 10.1016/j.envpol.2018.01.038.

[22] Juan Locutura Rupérez. *Atlas Geoquímico de España (Recursos minerales)*. Spanish Edition. Instituto Geológico y Minero de España, 2012. ISBN: ISBN10-8478408754.

[23] R. Calvo de Antaa E. Luísa M. Febrero-Bandeb J. Galiñanesa F. Macíasa R. Ortízc F. Casás. "Soil organic carbon in peninsular Spain: Influence of environmental factors and spatial distribution". In: *Geoderma vol 370* (2019). DOI: 10.1016/j.geoderma.2020.114365.

[24] THE COUNCIL OF THE EUROPEAN UNION. "COUNCIL DIRECTIVE 2013/59/EURATOM of 5 December 2013". In: *Official Journal of the EU* (2013).

[25] Robert C. Richter Dirk Link H. M. Kingston. "Microwave-Enhanced". In: *Analytical Chemistry* (2001). DOI: 10.1021/ac0123781.

[26] DOUGLAS SKOOG. *FUNDAMENTOS DE QUIMICA ANALITICA (8ª ED.)* Octava edition, 2005.

[27] Martin A. Blanchard R.L. "The thermal volatilisation of caesium-137, polonium-210 and lead-210 from in vivo labelled samples." In: *Analyst 94* (1969), pp. 441–446. DOI: 10.1039/an9699400441.

[28] R.M. Twyman. *Encyclopedia of Analytical Science (Second Edition): SAMPLE DISSOLUTION FOR ELEMENTAL ANALYSIS | Wet Digestion*. Science direct, 2005.

[29] Guogang Jia Giancarlo Torri. "Determination of 210Pb and 210Po in soil or rock samples containing refractory matrices". In: *Applied Radiation and Isotopes Volume 65* (2006), pp. 1–8. DOI: 10.1016/j.apradiso.2006.05.007.

[30] Ganzler K. Salgo A. "MICROWAVE EXTRACTION: A NOVEL SAMPLE PREPARATION METHOD FOR CHROMATOGRAPHY". In: *Journal of Chromatography, 371* (1986), pp. 299–306. DOI: 10.1016/s0021-9673(01)94714-4.

[31] Lucia Lopez-Hortas Maria D. Torres Herminia Dominguez. *Innovative and Emerging Technologies in the Bio-marine Food Sector: Chapter 15, Equipment and recent advances in microwave processing*. Elsevier, 2022, pp. 333–360. DOI: 10.1016/B978-0-12-820096-4.00009-2.

[32] Grupo GIDOLQUIM. *TÉCNICAS Y OPERACIONES AVANZADAS EN EL LABORATORIO QUÍMICO (TALQ)*. `https://www.ub.edu/talq/es/node/247`.

[33] W.W. Flynn. "THE DETERMINATION OF LOW LEVELS OF POLONIUM-210 IN ENVIRONMENTAL MATERIALS". In: *Analytica Chimica Acta Volume 43* (1968). DOI: `10.1016/S0003-2670(00)89210-7`.

[34] M.L.Jackson. *Soil Chemical Analysis*. Prentice Hall Inc, 2005.

[35] Saifeddine RAHALI. "Etude de polonium-210 dans le tabac consommé en Tunisie". PhD thesis. Université Tunis El Manar Faculté des Sciences de Tunis, 2013.

[36] J. Derrien. *Physique des détecteurs nucléaires*. Chapitre 3. Institut Supérieur d'Ingénieur de Bruxelles (ISIB). Belgique.

[37] PhD Ing. Isabelle Gerardy. *Métrologie nucléaire*. ISIB. 2020.

[38] Marina Sáez Muñoz. "Desarrollo de procedimientos rápidos de ensayo para la vigilancia radiológica ambiental en situaciones de emergencia." PhD thesis. Universitat Politècnica de València, 2019.

[39] S Tarjan. *Evaluation report for laboratory n°57*. IAEA. 2014.

[40] S Tarjan. *Individual Evaluation Report for Laboratory Nr. 179*. IAEA. 2018.

[41] Marina Sáez Muñoz. *INSTRUCCIÓN TÉCNICA PARA LA DIGESTIÓN DE MUESTRAS CON MICROONDAS Y FUSIÓN*. UPV/LRA. 2018.

[42] A Savidou K Kehagia K Eleftheriadis. "Concentration levels of 210Pb and 210Po in dry tobacco leaves in Greece". In: *Journal of Environmental Radioactivity Volume 85* (2005), pp. 94–102. DOI: `10.1016/j.jenvrad.2005.06.004`.

[43] A.C. Peres G. Hiromoto. "Evaluation of Pb-210 and Po-210 in cigarette tobacco produced in Brazil". In: *Journal of Environmental Radioactivity Volume 62* (2002), pp. 115–119. DOI: `10.1016/S0265-931X(01)00146-1`.

Part 2: Budget

1 Introduction

In the following section, we will carry out an economic evaluation of the costs attributed to this research work. To do this, we must first examine each part of the procedure. Both the materials and reagents consumed in each test and the wear and tear on the measuring equipment used must be evaluated. In addition, the personnel needed to carry out the tests and the personnel needed to analyse the results obtained must be taken into account. The points that have been taken into account when drawing up the project budget are listed below.

- **Personal**: The procedure for the determination of polonium in natural samples is a laboratory test that requires the skills of personnel with previous experience in the field. The process includes an experimental stage, during which the digestion of samples is performed and the preparation of Alpha sources by deposition is carried out. The prepared samples must then be measured. This experimental part of the test is performed by a laboratory technician. Finally, a supervising technician (group A or B) processes the data, performs the necessary calculations and analyses the results obtained. To account for the cost of the personnel involved in the project, the average annual gross fees of each worker according to their group must be taken into account. The real cost to the company of each of them is then calculated by applying the additional percentage of social security (29,1%) to be paid by the company. In this case, it is paid by the Radiation Service of the Polytechnic University of Valencia. Based on the monthly cost and the hours worked per month (150 h/month), the hourly cost of the personnel required to carry out the procedure is calculated. On the other hand, it is necessary to take into account the working hours required by each of the workers to carry out the project. Taking into account the percentage of dedication required for each of them, the total cost of the personnel involved in the project is calculated.

- **Equipment** With regard to the equipment needed to carry out the test, both the main alpha spectrometric measurement equipment and the auxiliary equipment used throughout the test and for its operation (vacuum pump, hot plate, etc.) should be considered. In order to allocate the cost of the equipment to the project, the depreciation period or useful life of the equipment should be considered. This is a way of economically assessing the consumption or wear and tear of the equipment due to its use. In this case, the equation 31 is applied to calculate the depreciation cost (A_m:

$$A_m = \frac{C \cdot n \cdot t}{T} \tag{31}$$

  With:

  - C acquisition cost of the equipment (€).
  - t duration of use of the equipment in the project (years).
  - n level of use of the equipment (in base 1).
  - T useful life period of equipment.

- **Fungibles** Consumable material is material that is consumed in the course of the research project. In this case, it can be subdivided into: reagents used, tracers, consumables and

other laboratory equipment. The first three are allocated a cost according to the quantity used in the project. On the other hand, laboratory equipment (glassware, filtration system, etc.) may be used repeatedly. To take this cost into account, a change of material every 1 to 3 years (depending on the specific type) has been assumed. The cost of each of these per test was then allocated, assuming that approximately 50 polonium tests can be performed per year. Finally, this figure was multiplied by the number of tests performed.

The detailed budget with all costs associated with the research project will be presented below. The different price tables will be presented for each type of cost (personnel, equipment and consumables) with the cost justification of all the elements that make them up.

2 Personal

Table 14 shows the hourly cost of each worker to the company. The final price table for the company's staff is presented below, taking into account the number of hours spent on the project and the percentage of dedication required for the type of work (Table 15).

Table 14: Hourly cost of staff for the company.

Personal	Gross fees (€/year)	Cost to comp. (€/year)	Cost to comp. (€/month)	h/month	Cost to comp. (€/h)
Laboratory Technician	20.663,18 €	26.676,17 €	2.223,01 €	150	14,82 €
Supervisor	23.684,86 €	30.577,15 €	2.548,10 €	150	16,99 €

Table 15: Price table for staff involved in the project

Personal	Cost to company (€/h)	Quantity (h/test)	Dedication	N°Test	Cost (€/Tes.)
Laboratory Technician	14,82 €	15	33%	33	2.420,86 €
Supervisor	16,99 €	2	100%	33	1.121,16 €
				TOTAL	3.542,02 €

3 Equipment

Table 16 shows the cost associated with the equipment used during the development of the project. It takes into account the equipment needed for the alpha spectrometry measurement and the rest of the auxiliary equipment used in the rest of the procedure. The depreciation period considered is 10 years for the microwave system and 6 years for the rest of the main equipment systems.

Table 16: Equipment

Equipment	Acqu. cost (€/unit)	Amort. time (years)	Time in use project (h)	Level of use	Cost (€)
Alpha Ensemble from ORTEC	21.380,00 €	6	10999,56	50%	558,91 €
Pfeiffer DUO 6 vacuum pump	1.600,00 €	6	2749,89	25%	15,85 €
Personal computer	1.000,00 €	6	2749,89	25%	9,91 €
Filtration pump Büchi Vac V-500	650,00 €	6	16,50	50%	0,08 €
Multi-place hotplate with agitation	952,00 €	6	660,00	33%	3,02 €
Scale	5.000,00 €	6	35,50	100%	1,19 €
Mutiwave go from Antoon Paar	20.000,00 €	10	66,00	100%	11,42 €
Ph meter	667,00 €	6	16,50	100%	0,16 €
				TOTAL	600,53 €

4 Fungibles

The costs of all consumables, i.e. reagents, tracer solution used and materials consumed or used up in the various tests of the project, are detailed below. The sum total of these costs will be the total cost of consumables.

4.1 Reagents

The following is a breakdown of the cost of reagents consumed in the project for the development of the procedure. It shows the consumption in ml or grams per test and the number of tests in which each reagent was consumed. Taking into account the unit price, this gives the total cost of the project (Table 17).

Table 17: Reagents

Reagents	Quantity	Acqu. cost (€)	Unit price (€/unit)	Cons. (mL or g/Test)	Nº Test	Cost (€)
Hydrochloric acid (37-38%), mL	1000	25,40	0,03	2	73	3,71
Nitric acid (65%), mL	1000	27,93	0,03	8	73	16,31
Ammonium hydroxide (25%), mL	1000	14,77	0,01	1	33	0,49
Hydroxylamine chloride, g	250	45,00	0,18	1	33	5,94
Hydrofluoric acid, ml	1000	27,90	0,03	2	73	4,07
Hydrogen peroxide, ml	1000	27,44	0,03	2	73	4,01
Bismuth, g	25	92,98	3,72	0,01	33	1,23
Sodium citrate, g	500	15,17	0,03	1	33	1,00
alcohol,ml	1000	3,95	0,00	10	33	1,30
Silver and metal cleaning cream, ml	250	2,30	0,01	5	33	1,52
					TOTAL	39,58 €

4.2 Tracer

During the development of the project, many tests were performed with the tracer Po-209. Below is an approximate calculation of the cost of using this tracer in relation to the initial cost of the primary tracer solution (Table 18). Taking into account the cost per Bq, the consumption per test and the number of tests in which each tracer is used, a unit price can be calculated.

Table 18: Tracer

Tracer	Activity (Bq)	Acqui. cost (€)	Disol. (Bq/mL)	Unit price (€/Bq)	Cons. (mL/tes.)	Nº Tests	Cost (€)
Po-209 solution	85,42	1.500,00 €	0,1885	17,56	0,3	33	32,77
						TOTAL	32,77

4.3 Fungible material

Table 19 shows the breakdown of the cost associated with the materials consumed during the procedure. The unit price of each of them is taken into account, by the consumption that was made in each test, and the number of tests in which they were used. Finally, the total cost of consumables consumed throughout the project is obtained. '

4.4 Others materials

In addition to consumables, there is another type of laboratory material that is not consumed in each test. In order to associate a cost with the wear and tear that this equipment may undergo,

Table 19: Fungible material

Material	Quantity	Acquisition cost (€)	Unit price (€/unit)	Level of use	Consumption (unit./as.)	Assays	Cost (€)
Filter paper Whatman 42	100	49,00	0,49	100%	1	33	16,17
Silver discs (25mm diameter)	100	1518,00	15,18	100%	1	33	500,94
Latex gloves	100	7,40	0,07	100%	6	33	14,65
						TOTAL	531,76

the acquisition cost was allocated in proportion to the years that each piece of equipment may last (between one and three years) and it was taken into account that up to 50 tests may be performed per year. This cost per test was multiplied by the number of tests to obtain the total cost of wear and tear for the whole project (Table 20).

Table 20: Others Materials

Material	Acqu. cost (€)	Quantity	Amortisation (years)	Cons. (cons./tes.)	Cost (€/ass.)	Cost (€)
Nahira filtration equipment	155,00	1	1	0,01	1,55	51,15
Teflon beaker	33,97	4	1	0,04	1,36	44,84
Glass beaker	1,00	4	1	0,04	0,04	1,32
Certified pipette 100-1000 µL	79,00	1	3	0,01	0,26	8,69
Certified pipette 20-200 µL	79,00	1	3	0,01	0,26	8,69
Automatic pipette	600,00	1	3	0,01	2,00	66,00
					TOTAL	180,69 €

5 Final budget

Once the cost associated with personnel, equipment and consumables is known, the actual cost of the whole project must be calculated. The first step is to calculate the Material Execution Budget (MEB), which is the sum of the total costs of the different elements mentioned above. However, the MEB does not take into account the overhead costs of electricity, water, furniture and additional equipment that are also consumed during the project. The overheads represent 15% of the MEB and are included in the investment budget. The investment budget is therefore the sum of the physical implementation budget and the cost associated with the overheads. Finally, 21% VAT must be applied to the investment budget to obtain the total project budget. It should be noted that this is a non-profit project, exclusively for the Polytechnic University of Valencia, specifically the UPV Environmental Radioactivity Laboratory. In this case, it would not be necessary to apply the additional cost due to the industrial benefit (6%), as it is not expected to obtain an economic benefit from the project. Finally, the budget would be as shown in Table 21.

Table 21: Final budget of the research project.

Concept		Total cost (€/Test)	
Staff		3.542,02 €	
Equipment		600,53 €	
Fungible (material, reagents, tracers, ...)		851,62 €	
Material Execution Budget (MEB)		**4.994,18 €**	
Material Execution Budget (MEB)		**4.994,18 €**	
Overheads (15%)	749,13 €		
		5.743,31 €	
Investment budget		**5.743,31 €**	
VAT (21%)	1.206,09 €		
TOTAL budget		**6.949,40 €**	

Therefore, the total budget for the project "Determination of Po-210 activity in natural samples by alpha spectrometry" amounts to:

Six thousand nine hundred and forty-nine euros and forty centimes

Valencia, June 2022
Belhadi Yassine

Part 3: Appendix

A   Methodology of the process

Method for natural sample :

Material and Equipment:

- Heating plate

- Rod stirrer

- Silver platelets, 25 mm diameter

- pH meter

- Filtration system

Reagents:

- Hydroxylamine hydrochloride, $(NH_3OH)Cl$, 20%. Dissolve 20 g in 100

ml distilled water

- Sodium citrate, $C6H_5O_7Na_3.2H_2O$, 25%. Dissolve 25 g in 100 ml of distilled

distilled water.

- Bismuth carrier (10 mg Bi^{3+}/ml). Dissolve 2,3211 g of

   $Bi(NO_3)_3.5H_2O$ in 5 ml of concentrated HNO_3

and dilute to 100 ml with distilled water.

- Certified standard solution of Po-209.

- Hydrochloric acid, a.s., HCl, 35 %.

- Ammonium hydroxide, s.s., NH_4OH, 25 %.

- Ethyl alcohol, 95 %.

Process:

A: Dryness

1. Collect a part of the sample
2. Dry the sample in the oven at 80°C for $\simeq 12h$

B: Microwave Digestion

1. Put in each vessel $\simeq 0,2$ g of the dry sample
2. Make the temperature calibration of the microwave
3. First step of digestion: programme ORGANIC B_LRA
   - Put 8 mL HNO_3, 2 mL HCl and 2 mL H_2O_2 in each vessel (be careful with H_2O_2, add it drop by drop)
   - Put the vessel in the rotor of the microwave
   - Ramp 15 min to 100°C

- 4 min at 100°C
- Ramp 15 min to 165°C
- 8 min at 165°C

4. Second step of digestion: programme HF
    - Open each vessel and put 2 ml HF
    - Rampa 10 min to 150°C
    - 5 min at 150°C

C: Evaporation and Filtration:

1. Put the solution from each vessel in a single Teflon beaker
2. Put the tracer (0,1 ml for contaminated sample and 0,5 ml for natural sample)
3. Heat at 80°C - 90°C to dryness
4. Add 2 ml of HCl and heat again at 80°C - 90°C to dryness (repeat this step 2 or 3 times)
5. Add 5 ml of demineralize water and 2 ml of HCl
6. Filtrate the solution with a cellulose filter (Filter papers 42 ashless diameter 55mm from GE healthcare life science Whatman) using the filtration system
7. Put the solution in a glass beaker

C: Deposition

1. Add 5 ml of Hydroxylamine Hydrochloride 20%
2. Add 2 ml of Sodium citrate 20%
3. Add 1ml of Bi carrier solution (concentration = 10mg/ml)
4. Adjust the pH at 2 with NH_4OH 25% or HCl 35% if necessary
5. Dilution to 50 ml with demineralize water
6. Put the solution in a Teflon beaker and put it on the Hot-plate magnetic stirrer
7. Heat at 85-90 °C + stir with Teflon stirrer (2-3 min)
8. Put the Silver disk in the beaker
9. Stir 75min at 85-90°C
10. Wash with demineralize water + Ethanol and dry
11. Count (alpha spectrometry)

B Inter-comparison sample MI38 information

M1-38/39/40

The IAEA-TEL-2012-03 worldwide open proficiency test

Laboratory No. 57, Results submitted on 2013-05-10

Evaluation Report

for

Laboratory No. 57

(revised April 2014)

Your personal customer number: 1631

Techical Director Josefina Ortiz

LABORATORIO RADIACTIVIDAD AMBIENTAL
*
UNIVERSITAT POLITECNICA DE VALENCIA*
Camino de Vera, S/N
*
46022 VALENCIA*
*
SPAIN*
ES

Tel: +34963877098
Fax: +34963877099
e-mail: jortiz@iqn.upv.es
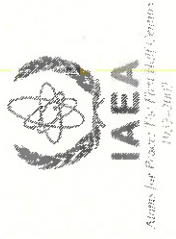
Contact Information

S. Tarjan
IAEA Reference Materials Group
Terrestrial Environment Laboratory
NA Environment Laboratories NAEL
International Atomic Energy Agency
A-2444 Seibersdorf - Austria

Email: s.tarjan@iaea.org

Tel: +43 1 2600 28242
Fax: + 43 1 2600 28222

http://nucleus.iaea.org/rpst/

IAEA
Atoms for Peace 1957-2007

The IAEA-TEL-2012-03 worldwide open proficiency test

Evaluation Criterias

The data is evaluated according to the following steps:

The relative bias between the reported and the target value (the best estimation of the true value) is expressed by the following equation:

$$Bias_{relative} = \frac{Value_{reported} - Value_{target}}{Value_{target}} \times 100\%$$

The relative bias will be compared to the Maximum Acceptable Relative Bias (**MARB**) which has been determined for each measurand, considering the physical background of radioanalytical methods, including the level of the radioactivity and the complexity of the task.

If the **Bias**$_{relative}$ ≤ **MARB** value the result will be "Accepted" for accuracy.

Based on fit for purpose and the good laboratory practice principles the expanded relative combined uncertainty should cover the relative bias:

$$P = 2\sqrt{\left(\frac{u_{target}}{A_{target}}\right)^2 + \left(\frac{u_{reported}}{A_{reported}}\right)^2} \times 100$$

$$Bias_{relative} \leq k * P$$

where k is the coverage factor, for the 95% confidential level k is 2.56. If the reported result is between the ± **MARB** values, but it is not overlapping with the target value within their uncertainties, this equation helps to decide whether they are significantly different or not.

The **P** value will be compared to the **MARB** also. If both the **P ≤ MARB** and **Bias**$_{relative}$ ≤ **k*P** are fulfilled the reported result will be "Accepted" for the precision. If one of them is insufficient the result will be assigned the "Not accepted" status for precision.

The final score according to the above detailed evaluation:
"**Accepted**" when both accuracy and precision achieved "Accepted" status,
"**Not Accepted**" when the accuracy is "Not accepted" and
"**Warning**" when accuracy is "Accepted", but the precision is "Not accepted".

The IAEA-TEL-2012-03 worldwide open proficiency test

Laboratory No. 57, Results submitted on 2013-05-10

Evaluation on Sample 4, Hay

Reference Date: 01-01-2012

Analyte	IAEA Value [Bq/kg d.m.]	IAEA Unc [Bq/kg d.m.]	Lab Value [Bq/kg d.m.]	Lab Unc [Bq/kg d.m.]	Lab Unc %	Rel. Bias %	u-Test	Ratio Lab/IAEA	Accuracy	P(%)	Precision	Final Score
Cs-134	316	20	310	11	3.55	-1.90	-0.26	0.98	A	7.26	A	A
Cs-137	815	24	857	21	2.45	5.15	1.32	1.05	A	3.83	A	A

Evaluation on Sample 5, Soil

Reference Date: 01-01-2012

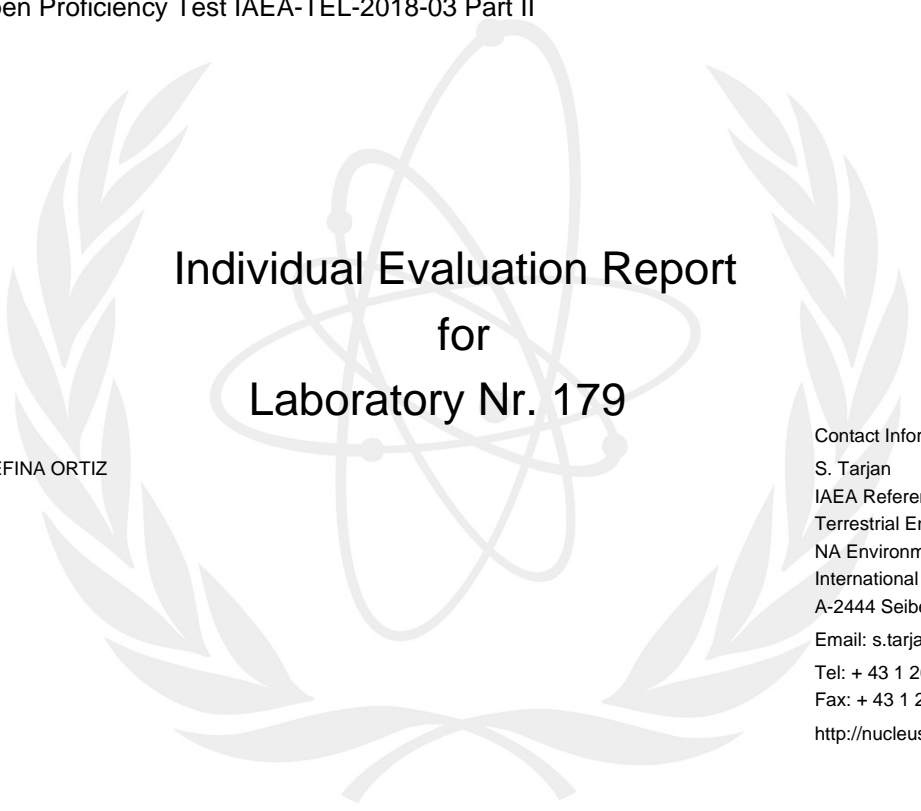| Analyte	IAEA Value [Bq/kg d.m.]	IAEA Unc [Bq/kg d.m.]	Lab Value [Bq/kg d.m.]	Lab Unc [Bq/kg d.m.]	Lab Unc %	Rel. Bias %	u-Test	Ratio Lab/IAEA	Accuracy	P(%)	Precision	Final Score
Ac-228	32.4	1.6	35	3	8.57	8.02	0.76	1.08	A	9.89	A	A
Am-241	1.78	0.1										
Cs-137	118.6	2.9	116	3	2.59	-2.19	-0.62	0.98	A	3.56	A	A
K-40	207.7	8.3	205	14	6.83	-1.30	-0.17	0.99	A	7.91	A	A
Pb-210	595	19	528	18	3.41	-11.26	-2.56	0.89	A	4.67	A	A
Pb-212	31.0	1.2	32.6	1.3	3.99	5.16	0.90	1.05	A	5.56	A	A
Po-210	573	25	529	17	3.21	-7.68	-1.46	0.92	A	5.42	A	A
Pu-239+240	4.74	0.1										
Sr-90	25.4	1.9	27	2	7.41	6.30	0.58	1.06	A	10.53	A	A
Tl-208	11.5	0.6	13.0	0.8	6.15	13.04	1.50	1.13	A	8.07	A	A
U-238	23.6	0.7	13.9	0.8	5.76	-41.10	-9.12	0.59	N	6.47	N	N

C   Inter-comparison sample MI67 information

Individual Evaluation Report

for the World-Wide Open Proficiency Test IAEA-TEL-2018-03 Part II

Individual Evaluation Report
for
Laboratory Nr. 179

Participant Information:

Technical Director JOSEFINA ORTIZ
Camino de Vera, s/n
46022
Valencia

Proficiency Test IAEA-TEL-2018-03 Evaluation Report Part II

Created on 2018-10-29

Evaluation Result Table for Sample 4

Sample Code	Analyte	Target Value	Target Unc.	MARB	Rep. Value	Rep. Unc	Rel. Bias	Robust SD	Z-Score	Accuracy	P	Precision	Final Score
4	Ac-228	32.6	1.3	25 %	38	2	16.56 %	2.3	2.35	A	6.60	A	A
4	Am-241	53.1	0.9	20 %	54.9	1.4	3.39 %	6.3	0.29	A	3.06	A	A
4	Ba-133	56.8	0.9	20 %	55.4	0.8	-2.46 %	5.9	0.24	A	2.14	A	A
4	Bi-214	31.2	1.5	20 %	28	1	-10.26 %	5.8	0.55	A	5.99	A	A
4	Co-60	141.8	2.7	20 %	134.5	0.9	-5.15 %	8.3	0.88	A	2.02	A	A
4	Cs-134	112.2	1.6	20 %	109.7	0.9	-2.23 %	9.1	0.27	A	1.65	A	A
4	Cs-137	64.9	1.2	20 %	63.9	0.8	-1.54 %	4	0.25	A	2.23	A	A
4	K-40	374	15	20 %	413	24	10.43 %	32.8	1.19	A	7.06	A	A
4	Pb-210	485	11.6	20 %	504	19	3.92 %	82.9	0.23	A	4.46	A	A
4	Pb-212	32.6	1.3	25 %	33	1	1.23 %	3.1	0.13	A	5.01	A	A
4	Pb-214	31.2	1.5	20 %	28.7	1.2	-8.01 %	3.4	0.74	A	6.37	A	A
4	Ra-226	31.2	1.5	20 %	28.7	1.2	-8.01 %	19	0.13	A	6.37	A	A
4	Tl-208	11.7	0.4	25 %	10.6	0.8	-9.40 %	1.3	0.85	A	8.29	A	A
4	U-234	25	1.7	20 %	25.90	1.16	3.60 %	5.8	0.16	A	8.14	A	A
4	U-235	1	0.1	30 %	0.93	0.09	-7.00 %	0.4	0.18	A	13.92	A	A
4	U-238	25	1.7	20 %	26.59	1.19	6.36 %	5.8	0.27	A	8.14	A	A